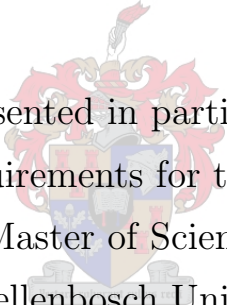


Electromagnetic Production of Mesons and Hyperons from Nuclei

Tony Nsio Nzundu



Thesis presented in partial fulfilment
of the requirements for the degree of
Master of Science
at Stellenbosch University

Supervisor: Dr B. I. S. Van Der Ventel

Co-Supervisor: Prof G. C. Hillhouse

December 2007

Declaration

I, the undersigned, hereby declare that the work contained in this thesis is my own original work and has not previously, in its entirety or in part, been submitted at any university for a degree.

Tony Nsio Nzundu

Date

Abstract

A relativistic plane wave model is developed for electromagnetic production of unbound hyperons with free kaons from nuclei. The differential cross section is expressed as a contraction of leptonic and hadronic tensors. The leptonic tensor is constructed by using the helicity representation of a free Dirac spinor. A model for the corresponding elementary process is used to calculate the hadronic tensor, in which the hadronic current operator \hat{J}^μ is written as a linear combination of six invariant amplitudes and six Lorentz and gauge invariant quantities. The kinematics for this process is assumed to be a quasi-free process i.e., the electron interacts with only one bound nucleon inside the nucleus. The bound state wavefunction of the bound nucleon is calculated within the framework of the relativistic mean-field approximation. The unpolarized differential cross section for the K^+ electroproduction process, $e + A \longrightarrow e + K^+ + \Lambda + A_{residual}$ is calculated as a function of the hyperon scattering angle.

Opsomming

Die elektromagnetiese produksie van mesone en vrye hiperone word bestudeer deur gebruik te maak van 'n relativistiese vlakgolf model. Die differensiële kansvlak word geskryf as die kontraktsie van 'n leptoniese en 'n hadroniese tensor. Die leptoniese tensor word bereken deur gebruik te maak van die helisiteitsvoorstelling van die vrye Dirac spinore. 'n Model vir die ooreenstemmende elementêre verstrooiingsproses word gebruik om die hadroniese tensor te bereken. Die hadroniese stroomoperator J^μ word uitgebrei in terme van ses Lorentz- en ykinvariante hoeveelhede. Daar word aanvaar dat die reaksie verloop volgens kwasievrye kinematika, met ander woorde die elektron wisselwerk slegs met een gebonde nukleon in die nukleus. Die golffunksie vir die gebonde nukleon word bereken deur gebruik te maak van die relativistiese gemiddelde veld benadering. Die nie-gepolariseerde kansvlak vir die K^+ elektromagnetiese proses, $e + A \longrightarrow e + K^+ + \Lambda + A_{residual}$ word bereken as funksie van die hiperon se verstrooiingshoek.

Dedication

This thesis is dedicated to my Lord Jesus Christ for all he has provided me with. He is my only spiritual support.

I also dedicate this work to:

- my late lamented father *Michèl* Nsio Mfumu Munankie and my ambitious mother *Collète* Ngamba Makiebe for all their family commitments.
- my sisters and brothers for their support, encouragement and prayers.
- my delightful wife *Dédé* Miyila Kiese who provides me with all her support and understanding to fulfill my dream.
- my friends and colleagues which support me in this dream.

Last but not least, my sincere thanks goes also to my brother and friend Mr *Paul* Nsio Ngamba for everything you have done to my life.

Acknowledgments

My first and deepest expression of gratitude goes to Dr Brandon Van Der Ventel and Professor Greg Hillhouse for providing me with all their knowledge, expertise and assistance. I also want to thank all my colleagues in the nuclear physics group at the Physics Department of Stellenbosch University for their exceptional contribution, discussion and help in the final stage of this work. I also acknowledge financial support from the African Institute for Mathematical Sciences, the Physics Department of Stellenbosch and the National Research Foundation.

Contents

1	Introduction	1
1.1	Motivations and Objectives	2
1.2	Outline of the thesis	5
2	Generalities	6
2.1	Scattering Process	6
2.1.1	Electron Scattering	7
2.1.2	Scattering Matrix Element	8
2.2	Electromagnetic Interaction	9
2.2.1	Electromagnetic Field and Potentials	9
2.3	Lorentz Gauge	10
2.4	Free Dirac Spinor	11
2.4.1	Dirac Equation	11
2.4.2	The helicity representation of the Free Dirac Spinor	13
2.5	Bound state wavefunction	14
3	Quasifree Electroproduction of Mesons from Nuclei	19

3.1	Schematic picture	19
3.2	Basic ingredients	20
3.3	Cross section for pseudoscalar-meson electroproduction	21
3.4	The kinematics	22
3.5	Dynamics of the process	24
3.5.1	Leptonic tensor	25
3.5.2	Hadronic tensor	26
3.6	Nuclear Structure	28
3.7	Bound State Propagator	33
4	Results	38
4.1	Kinematic setup	38
5	Summary and Conclusions	52
	Appendices	54
A	Derivation of the Differential Cross section	54
B	Leptonic tensor	61
C	The Hadronic tensor	64

List of Figures

2.1	Electron-proton elastic scattering process	7
2.2	Lowest-order Feynman diagram for an elastic scattering between a free electron and free proton	9
2.3	Upper and lower radial wave function $g(r)$ and $f(r)$ for the orbitals $1s_{1/2}$ and $1p_{3/2}$ of ^{12}C and the orbitals $1s_{1/2}$, $1p_{1/2}$ and $1p_{3/2}$ of ^{16}O	16
2.4	Upper and lower radial wave function $g(r)$ and $f(r)$ for the orbitals $1s_{1/2}$, $2s_{1/2}$, $1p_{3/2}$, $1p_{1/2}$, $1d_{5/2}$, $1d_{3/2}$ of ^{40}Ca and the orbitals $1s_{1/2}$, $2s_{1/2}$, $1p_{3/2}$, $1p_{1/2}$, $1d_{5/2}$, $1d_{3/2}$ of ^{208}Pb	17
2.5	Upper and lower radial wave function $g(r)$ and $f(r)$ for the orbitals $3s_{1/2}$, $2p_{1/2}$, $2p_{3/2}$, $2d_{5/2}$, $2d_{3/2}$ of ^{208}Pb and the orbitals $1h_{11/2}$, $1g_{9/2}$, $1g_{7/2}$, $1f_{7/2}$, $1f_{5/2}$ of ^{208}Pb	18
3.1	Lowest order Feynman diagram for the electroproduction of mesons and hyperons from nuclei	20
3.2	The coordinate system of the reaction $A(e, e K^+ \Lambda)A_{\text{res}}$ in the laboratory frame	22
3.3	Approximation employed at the hadronic vertex in order to obtain a tractable form of the matrix element for the electromagnetic production of meson and unbound hyperon from the single bound nucleon.	27

3.4	Upper $g(p)$ and lower $f(p)$ component of the radial bound state wave-function of the bound nucleon in the momentum space representation for the orbitals $1s_{1/2}$ and $1p_{3/2}$ of ^{12}C and $1s_{1/2}$, $1p_{1/2}$ and $1p_{3/2}$ of ^{16}O	30
3.5	Upper $g(p)$ and lower $f(p)$ component of the radial bound state wave-function of the bound nucleon in the momentum space representation for the orbitals $1s_{1/2}$, $2s_{1/2}$, $1p_{3/2}$, $1p_{1/2}$, $1d_{5/2}$, $1d_{3/2}$ of ^{40}Ca and $1s_{1/2}$, $2s_{1/2}$, $1p_{3/2}$, $1p_{1/2}$, $1d_{5/2}$, $1d_{3/2}$ of ^{208}Pb	31
3.6	Upper $g(p)$ and lower $f(p)$ component of the radial bound state wave-function of the bound nucleon in the momentum space representation for the orbitals $3s_{1/2}$, $2p_{1/2}$, $2p_{3/2}$, $2d_{5/2}$, $2d_{3/2}$ of ^{208}Pb and $1h_{11/2}$, $1g_{9/2}$, $1g_{7/2}$, $1f_{7/2}$, $1f_{5/2}$ of ^{208}Pb	32
3.7	The effective mass-, energy, and momentum-like quantities: M_α , E_α and \mathbf{p}_α as a function of the momentum (p)	34
3.8	The effective mass-, energy, and momentum-like quantities: M_α , E_α and \mathbf{p}_α as a function of the momentum (p)	35
3.9	The radial component $g_\alpha(p)$ and $f_\alpha(p)$ of the wave function of the bound-nucleon (proton in our case) in momentum space for orbital $1p_{3/2}$ of the ^{12}C nucleus	36
4.1	Upper $g(p)$ and lower $f(p)$ components of the proton bound state wave-function in the momentum space for the orbitals $1s_{1/2}$ and $1p_{3/2}$ of ^{12}C for $E_{K^+}=700$ MeV and 720 MeV	41
4.2	Upper $g(p)$ and lower $f(p)$ components of the proton bound state wave-function in the momentum space for the orbitals $1s_{1/2}$, $1p_{3/2}$ and $1p_{1/2}$ of ^{16}O for $E_{K^+}=700$ MeV and 720 MeV	42
4.3	The differential cross section for the electro-production of K^+ and unbound hyperon using the orbital $1s_{1/2}$ of the ^{12}C nucleus	44

-
- 4.4 The differential cross section for the electro-production of K^+ and unbound hyperons using the orbital $1p_{3/2}$ of the ^{12}C nucleus 45
- 4.5 Differential cross section for the K^+ electro-production with free hyperon from the ^{12}C nucleus (top), using the orbital $1s_{1/2}$ and $1p_{3/2}$, and ^{16}O (bottom), the orbital $1s_{1/2}$ and $1p_{3/2}$ using the orbital $1s_{1/2}$, $1p_{3/2}$ and $1p_{1/2}$ for different energies transfer ω 46
- 4.6 Differential cross section for the K^+ electro-production with free hyperon from the ^{40}Ca nucleus, using the orbital $1s_{1/2}$, $1p_{3/2}$, $1p_{1/2}$ (top), and using the orbital $1d_{5/2}$, $1d_{3/2}$ and $2s_{1/2}$ (bottom), for different energies transfer ω 48
- 4.7 Differential cross section for the K^+ electro-production with free hyperon from the ^{208}Pb nucleus, using the orbital $1s_{1/2}$, $1p_{3/2}$, $1p_{1/2}$, $1d_{5/2}$, $1d_{3/2}$ and $2s_{1/2}$ for different energies transfer ω 50
- 4.8 Differential cross section for the K^+ electro-production with free hyperon from the ^{208}Pb nucleus, using the remaining orbitals from $1f_{7/2}$ to $3s_{1/2}$ in the shell structure for different energies transfer ω 51

List of Tables

1.1	Quark content and masses of kaon, pion and eta pseudo-scalar mesons. . .	2
4.1	Acceptable kinematics	39
4.2	Shell structure parameters of ^{12}C for relativistic mean-field model	43
4.3	Shell structure parameters of the ^{16}O for relativistic mean-field model . . .	45
4.4	Shell structure parameters of ^{40}Ca for relativistic mean-field model	47
4.5	Shell structure parameters of ^{208}Pb for relativistic mean-field model	49

Chapter 1

Introduction

The essential goal of physicists has focused on the fundamental building blocks of matter, and to establish the properties of the constituents of matter, as well as to investigate the forces through which they interact. The electron was the first building block of the atom to be identified in 1897 by Thomson, by producing electrons as beams of free particles in discharge tubes. The discovery of the electron and radioactivity marked the beginning of a new era in the investigation of matter. At this time the atomic structure of matter was already visible. These discoveries began to shed light on the structure of matter. However, the full picture turned out to be much more complicated than had been imagined [1, 2]. The modern view is that three types of fundamental particles (*leptons, quarks and gauge bosons*) form the building blocks of matter. These particles interact via forces carried by exchange bosons: gluons for strong interactions (QCD), the photon for electromagnetic interactions (QED) and W^\pm, Z^0 bosons for weak interactions [3, 4, 5].

Mesons were originally predicted as carriers of the force that bind protons and neutrons. When first discovered, the muon was identified with this family from its similar mass and was named “ μ -meson”, however it did not show a strong attraction to nuclear matter and is actually a lepton. The pion was the first true meson to be discovered. In 1949 Hideki Yukawa was awarded the Nobel Prize in Physics for predicting the existence of the meson [1, 4].

A meson is a particular type of fundamental particle which is made up of a quark and an anti-quark. Today physicists define quarks as the elementary particles which constitute

fundamental building blocks of matter. Pseudoscalar mesons form a subgroup of mesons that have zero spin (namely scalars) and behave in a particular fashion under the action of symmetry operations, that is they have parity $P = -1$ [6, 7, 8]. Under the symmetry operation of spatial inversion the pseudoscalar meson wavefunction ϕ transforms to $-\phi$. Table: 1.1 illustrates the quark content of different states of the pseudoscalar mesons (as pion (π), eta (η), and kaon (K)) [9].

Pseudo-scalar Meson	Quark content	Mass (MeV/c ²)
Kaon	$K^+ \approx \bar{s}u$	493.677 ± 0.016
	$K^- \approx s\bar{u}$	493.677 ± 0.016
	$K^0 \approx \bar{s}d$	497.648 ± 0.022
	$\bar{K}^0 \approx \bar{d}s$	497.648 ± 0.022
Pion	$\pi^+ \approx \bar{d}u$	139.57018 ± 0.00035
	$\pi^- \approx d\bar{u}$	139.57018 ± 0.00035
	$\pi^0 \approx (u\bar{u} - d\bar{d})/\sqrt{2}$	134.9766 ± 0.0006
Eta	$\eta \approx (u\bar{u} + d\bar{d} - 2\bar{s}s)/\sqrt{6}$	547.51 ± 0.18

TABLE. 1.1. Quark content and masses of kaon, pion and eta pseudo-scalar mesons.

1.1 Motivations and Objectives

The production of mesons from nuclei is an established field of research in nuclear and particles physics. Both theoretical and experimental studies of mesons and their interactions with nucleons have been of great interest for nuclear and particles physics research in recent years [10, 11, 12, 13]. In this work we develop a theoretical model for analyzing the exclusive, quasifree electroproduction of pseudoscalar-mesons from nuclei, denoted

symbolically by

$$e + A \longrightarrow e + PS + \Lambda + A_{\text{res}} , \quad (1.1)$$

where PS can be one of the pseudoscalar mesons illustrated in Table. 1.1. The name “quasifree” refers here to the process that occurs in kinematic and physical circumstances similar to those of the process that produces a meson from a free unbound nucleon, and “exclusive” means that the outgoing particles are detected in coincidence [11, 14]. This allows one to consider just one bound nucleon in the nucleus and all others are viewed as spectators. This means that the process can be considered as taking place on a single nucleon inside the nucleus [15, 16]. The basic picture of this process is the follows: A virtual photon emitted by the electron beam, penetrates the target nucleus and couples to an individual nucleon via the latter’s charge and magnetic moment. This coupling causes oscillation of the nucleon, followed by the expulsion of kaons. The produced K-mesons, along with the nucleons that also exit the system, subsequently rescatter from the remaining nucleons before finally escaping and reaching the detector [17, 18]. The understanding of the way in which the kaon is produced from a bound nucleon, namely the photoproduction of the kaon from a single nucleon must be well known. Electroproduction describes a process where elementary particles are produced as a result of the action of an incident electron interacting with a target nucleus via exchange of virtual photons (electromagnetic waves) [10, 11, 19, 20]. In our model, the incident electron is assumed to interact with only one bound nucleon. As a result, a pseudoscalar meson is produced along with other particles. In this picture the meson is produced in association with a nucleon (or an excited state of the nucleon such as a lambda hyperon) and some new recoil “daughter” nucleus. Starting with an incident electron and some nucleus, we end up with an outgoing electron, a meson, a free nucleon (or an excited state of it), and a new (residual) nucleus.

The study of the above interactions provides an understanding of the fundamental strong force which plays an important role in interactions between elementary particles at very small distance scales [11, 14, 16]. There are four forces that drive all interactions in nature: gravitational, electromagnetic, weak, and strong forces. At present, we have a good understanding of the nature of the electromagnetic and the weak forces, while the gravitational and strong forces still elude a satisfactory and complete description [21, 22].

Many papers [12, 23, 24] are available on photoproduction of pseudoscalar mesons, in which the use of a real photon beam is employed. Recently η photoproduction from nuclei has

been studied via the reaction $A(\gamma, \eta N)B$ in the quasifree regime [25, 26, 27].

One of the goals in our study of the reaction in Eq. (1.1), is to illuminate our understanding of multiple areas of nuclear physics research such as meson-nucleon and the nucleon-nucleus interactions, quasi-free electron scattering from nuclei and also the electromagnetic production of mesons from nucleons [2, 13].

The electroproduction of pseudoscalar mesons from nuclei has not been studied in detail, and very few papers in this subject are available. The use of electrons instead of photons has the added the advantage of probing the longitudinal response and longitudinal-transverse response, but with the price of dealing with a more complicated structure in the cross section [11, 16, 21, 28]. Our hope is that in the near future experimental data will be available in order to confront our theoretical understanding with the experimental results. In developing our formalism we will use as guidance studies of the electroproduction of pions from nuclei, specifically the reaction: $A(e, e \pi N)B$ [11, 29].

The use of the Feynman diagrams and rules helps us to compute the transition matrix element employing the helicity representation of the Dirac spinor. We also find a detailed expression for the leptonic tensor, in which all kinds of situations are taken into account for massive and massless leptons. A canonical model-independent parameterization is used for the elementary process $\gamma N \longrightarrow K^+ \Lambda$. This parameterization is constructed in terms of a linear combination of six invariant amplitudes and six Lorentz- and gauge-invariance quantities. Because of the pseudoscalar nature of the K^+ meson, the transition matrix element is expanded using the well known Chew-Goldberger-Low-Nambu (CGLN) amplitudes [7, 30, 31]. The spin dependence is expressed via the hadronic current operator \hat{J}^μ produced by the strongly interacting hadron in terms of Lorentz covariant pseudo-vectors. The bound state wave function of the bound nucleon is calculated within the framework of the relativistic mean field approximation to the Walecka model.

The main objective of this work is to study quasifree electroproduction of the K^+ meson or Λ -hyperon from nuclei. The kinematics for this process is to be assumed as a quasifree kinematics i.e., the electron interacts with only one bound nucleon inside the nucleus. The unpolarized differential cross section for the K^+ electro-production process, $e + A \longrightarrow e + K^+ + \Lambda + A_{residual}$ is calculated as function of the hyperon scattering angle.

1.2 Outline of the thesis

This thesis is divided into five chapters. After the introduction, chapter two explains general concepts in the investigation of electromagnetic interactions between particles. In chapter three we discuss the formalism and the basic ideas of the quasifree electromagnetic production of mesons and unbound hyperon from nuclei. Here we will also briefly discuss the Relativistic Mean Field (RMF) model which incorporates nuclear structure aspects of our problem. We also concentrate on the derivation of the differential cross section and show that the transition matrix element can be written as a contraction of the leptonic and hadronic tensors. The leptonic tensor is derived using the helicity representation of the free Dirac spinor wavefunction. The bound state wavefunction is used in the calculation of the hadronic tensor taking into account nuclear structure for the hadronic current operator. In the fourth chapter we present the results of our theoretical investigation while the summary and conclusions are presented in chapter five.

Chapter 2

Generalities

In this chapter we review some basic concepts used in the treatment of interactions between particles. We also review some basic ideas about the electromagnetic field, since we will be focussing on electromagnetic production. The importance of the Dirac equation in the treatment of our model comes from the fact that we will be dealing with fermions. The bound state wave function will be introduced in order to describe the behaviour of the bound nucleon inside the nucleus.

2.1 Scattering Process

Scattering presents a useful tool for the investigation of interactions between particles [32]. In our scattering process we have the leptonic part represented by the incident and scattered electron on one side and the hadronic part represented by the target nucleus, the produced kaon and the Λ -hyperon on the other side. Here we illustrate this concept by considering a simple two-body scattering process [33].

Let us consider the following process,

$$e + p \rightarrow e + p, \tag{2.1}$$

whereby an electron (e) scatters elastically from a proton (p). Fig. 2.1 describes this process, in which we have assumed the laboratory framework, i.e., the target proton is at the rest, and hence its three-momentum is zero. We also assume for simplicity that

all particles involved in this process are unpolarized. The angle θ_e represents the electron scattering angle and ϕ is the azimuthal angle.

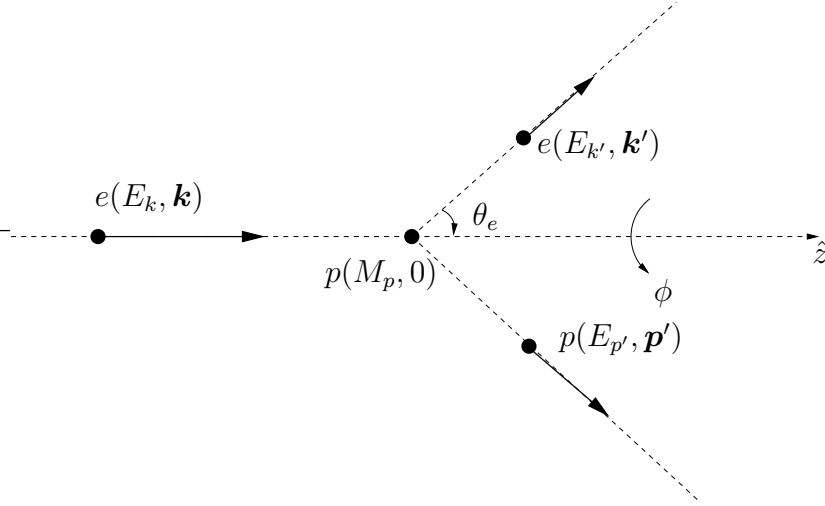


FIG. 2.1. Electron-proton elastic scattering process

2.1.1 Electron Scattering

Electron scattering is probably the best tool for investigating the structure of hadronic systems such as atomic nuclei and their constituents. The electromagnetic interaction is known from quantum electrodynamics (QED) and is weak compared with strength of the interaction between hadrons. Thus electron scattering is adequately treated assuming the validity of the Born approximation i.e., the one-photon exchange mechanism between electron and the target.

Let us consider Fig. 2.1, where an electron beam with four-momentum $k = (E_k, \mathbf{k})$ in the laboratory frame is incident on a rest proton target with four-momentum $p = (M_p, 0)$. If the incident electron e is scattered through an angle θ_e to the outgoing electron e with the four-momentum $k' = (E_{k'}, \mathbf{k}')$, due to the relative weakness of the electromagnetic interaction, the electron scattering can be treated as the exchange of a virtual photon which carries energy $\omega = E_k - E_{k'}$ and three-momentum $\mathbf{q} = \mathbf{k} - \mathbf{k}'$. Then the four-momentum transfer is given by $q = k - k' = (\omega, \mathbf{q})$. The four-momentum transfer squared

is space-like (invariant) and given by

$$q^2 = \omega^2 - |\mathbf{q}|^2 = -4E_k E_{k'} \sin^2 \frac{\theta_e}{2}. \quad (2.2)$$

We can also define the quantity

$$Q^2 = -q^2 \geq 0. \quad (2.3)$$

Here we have made use of the ultra-relativistic limit, where the electron mass m_e is very small with respect to its energy E , and therefore can be neglected. According to the kinematics of this process, momentum conservation law can be written as

$$\mathbf{k} = \mathbf{k}' + \mathbf{p}', \quad (2.4)$$

and energy conservation given by

$$E_k + M_p = E_{k'} + E_{p'}. \quad (2.5)$$

One can use the above equations to calculate all kinematical quantities of the process [34]. But since we have different situations before and after the collision, the investigation of the dynamics of this process needs the incorporation of a new quantity which gives us all information about the way in which the interaction between the initial states and final states occurs. This quantity is called the scattering transition matrix element. There is no exact expression for this quantity, nevertheless the use of Feynman diagrams greatly helps us to evaluate it in some approximate manner.

2.1.2 Scattering Matrix Element

The scattering (*transition*) matrix element contains all dynamical information of the scattering. In electroproduction for example, this gives information about nuclear structure, and also the nuclear effect responsible for the production of mesons and other particles. Feynman diagrams remain a useful pictorial technique for analysing elementary particle interactions. As an example, Fig. 2.2 represents the Feynman diagram for electron-proton elastic scattering.

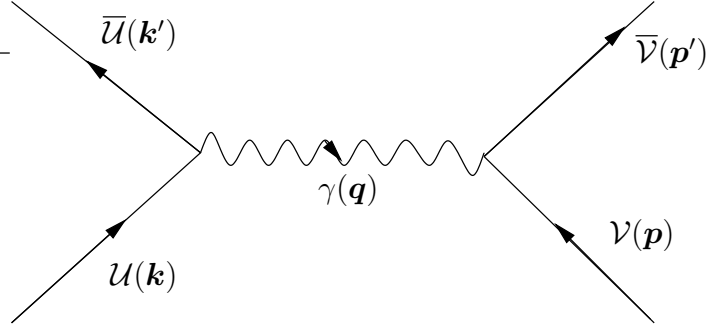


FIG. 2.2. Lowest-order Feynman diagram for an elastic scattering between a free electron and free proton

In this figure, $\mathcal{U}(\mathbf{k})$ represents the wavefunction of the incident electron with four momentum k , while the outgoing electron is represented by $\bar{\mathcal{U}}(\mathbf{k}')$ with momentum k' . The proton target is represented by $\mathcal{V}(\mathbf{p})$ and the recoil proton is represented by $\bar{\mathcal{V}}(\mathbf{p}')$. Here we have used the simplest mechanism to illustrate the usefulness of Feynman diagrams. In the framework of the Relativistic Plane Wave Impulse Approximation, the expression of the transition matrix element for this simplest Feynman diagram can be written as

$$\mathcal{M} \approx [\bar{\mathcal{U}}(\mathbf{k}') \gamma_\mu \mathcal{U}(\mathbf{k})] \frac{1}{q^2} [\bar{\mathcal{V}}(\mathbf{p}') J^\mu \mathcal{V}(\mathbf{p})], \quad (2.6)$$

where J^μ represents the proton current operator.

2.2 Electromagnetic Interaction

In this section we present the basic formalism for the description of the electromagnetic field and its interaction with hadronic matter for real and virtual photons [35].

2.2.1 Electromagnetic Field and Potentials

The complete description of the interaction between charged particles and the electromagnetic field can be made by controlling the scalar potential V_s and the vector potential \mathbf{V}_v . The electric and magnetic fields are given in a unique way using the above potentials

through the equations

$$\begin{aligned} \mathbf{E} &= -\nabla V_s - \frac{\partial \mathbf{V}_v}{\partial t}, \\ \mathbf{H} &= \nabla \times \mathbf{V}_v. \end{aligned} \quad (2.7)$$

However, for a variety of scalar and vector potentials, one can describe the fields \mathbf{E} and \mathbf{H} when the charge and current densities ρ_c and j_c are given [2, 36].

2.3 Lorentz Gauge

The transformation which leaves unchanged the equations in Eq. (2.7), is known as a gauge transformation, i.e.

$$\begin{aligned} V'_s(t, \mathbf{r}) &= V_s(t, \mathbf{r}) - \frac{\partial \lambda(t, \mathbf{r})}{\partial t}, \\ \mathbf{V}'_v(t, \mathbf{r}) &= \mathbf{V}_v(t, \mathbf{r}) + \nabla \lambda(t, \mathbf{r}). \end{aligned} \quad (2.8)$$

With the right choice of the function $\lambda(t, \mathbf{r})$, one can satisfy the Lorentz condition

$$\frac{\partial V_s}{\partial t} + \nabla \cdot \mathbf{V}_v = 0, \quad (2.9)$$

dealing with potentials which are solutions to the following Maxwell equations

$$\begin{aligned} \left(\frac{\partial^2}{\partial t^2} - \nabla^2 \right) V_s &= \rho_c \\ \left(\frac{\partial^2}{\partial t^2} - \nabla^2 \right) \mathbf{V}_v &= j_c. \end{aligned} \quad (2.10)$$

Hence, the Maxwell equations and the Lorentz condition are written as

$$\begin{aligned} \left(\frac{\partial^2}{\partial t^2} - \nabla^2 \right) V^\mu &= j_c^\mu \\ \partial_\mu V^\mu &= 0, \end{aligned} \quad (2.11)$$

where the four-vector potential V^μ is defined as

$$V^\mu(x) = V^\mu(t, \mathbf{r}) = (V_s, \mathbf{V}_v), \quad (2.12)$$

and $j_c^\mu = (\rho_c, j_c)$ is the four-vector current density.

2.4 Free Dirac Spinor

2.4.1 Dirac Equation

In quantum mechanics we define the Dirac equation as a relativistic wave equation describing an elementary spin- $\frac{1}{2}$ particle such as an *electron* in an electromagnetic field, whereby the wavefunction has four components. In natural units the Dirac equation without a potential (free equation) can be written as

$$i\frac{\partial\psi}{\partial t} = \hat{H}_f\psi = (\boldsymbol{\alpha} \cdot \hat{\mathbf{p}} + m\beta)\psi, \quad (2.13)$$

where \hat{H}_f is the free Hamiltonian [37, 38], m is the rest mass of the particle, where

$$\hat{\mathbf{p}} = -i\nabla, \quad (2.14)$$

is the three dimensional momentum operator and $\psi(t, \mathbf{x})$ is a four component wavefunction, and the 4×4 matrices $\boldsymbol{\alpha}$ and β are given by

$$\boldsymbol{\alpha} = \begin{pmatrix} 0 & \boldsymbol{\sigma} \\ \boldsymbol{\sigma} & 0 \end{pmatrix} \quad \text{and} \quad \beta = \begin{pmatrix} 1 & 0 \\ 0 & -1 \end{pmatrix}. \quad (2.15)$$

Equation Eq. (2.13) has solutions

$$\psi_\lambda(t, \mathbf{x}) = \psi(\mathbf{x})e^{-i\lambda Et}, \quad (2.16)$$

where $\lambda = \pm 1$, and then

$$\hat{H}_f\psi = i\psi(\mathbf{x})(-i\lambda E)e^{-i\lambda Et} = \lambda E\psi. \quad (2.17)$$

Splitting the 4-component spinors into two-2-component spinors ϕ and χ gives

$$\psi = \begin{pmatrix} \psi_1 \\ \psi_2 \\ \psi_3 \\ \psi_4 \end{pmatrix} = \begin{pmatrix} \phi \\ \chi \end{pmatrix}, \quad (2.18)$$

where

$$\phi = \begin{pmatrix} \psi_1 \\ \psi_2 \end{pmatrix} \quad \text{and} \quad \chi = \begin{pmatrix} \psi_3 \\ \psi_4 \end{pmatrix}. \quad (2.19)$$

Substitution into the free Dirac Equation, Eq. (2.13), gives

$$\lambda E \phi = \boldsymbol{\sigma} \cdot \hat{\mathbf{p}} \chi + m \phi, \quad (2.20)$$

and then

$$\lambda E \chi = \boldsymbol{\sigma} \cdot \hat{\mathbf{p}} \phi - m \chi. \quad (2.21)$$

States with definite momentum can be written as

$$\begin{pmatrix} \phi \\ \chi \end{pmatrix} = \begin{pmatrix} \phi_0 \\ \chi_0 \end{pmatrix} e^{i\mathbf{p} \cdot \mathbf{x}}, \quad (2.22)$$

which are eigenfunctions of the momentum operator

$$\hat{\mathbf{p}} \psi_{p\lambda}(t, \mathbf{x}) = \mathbf{p} \psi_{p\lambda}(t, \mathbf{x}). \quad (2.23)$$

Equations Eq. (2.20) and Eq. (2.21) become

$$(\lambda E - m) \phi_0 - \boldsymbol{\sigma} \cdot \mathbf{p} \chi_0 = 0, \quad (2.24)$$

and

$$-\boldsymbol{\sigma} \cdot \mathbf{p} \phi_0 + (\lambda E + m) \chi_0 = 0. \quad (2.25)$$

The solution requires that

$$\lambda^2 E^2 - m^2 - (\boldsymbol{\sigma} \cdot \mathbf{p})^2 = 0. \quad (2.26)$$

Finally, we have that

$$E = \frac{1}{\lambda} \sqrt{m^2 + p^2}, \quad (2.27)$$

where we have used the fact that $(\vec{\sigma} \cdot \mathbf{p})^2 = p^2$. One must be careful with the sign of λ when solving both cases at once.

We also have that

$$\phi_0 = \frac{\boldsymbol{\sigma} \cdot \mathbf{p}}{\lambda E + m} \chi_0, \quad \text{or} \quad \chi_0 = \frac{\boldsymbol{\sigma} \cdot \mathbf{p}}{\lambda E - m} \phi_0, \quad (2.28)$$

and let us denote the two-component spinor χ_0 by

$$\chi_0 = \mathcal{U} = \begin{pmatrix} u_1 \\ u_2 \end{pmatrix},$$

where u_1 and u_2 are complex and \mathcal{U} is normalized according to

$$\mathcal{U}^\dagger \mathcal{U} = u_1^* u_1 + u_2^* u_2 = 1. \quad (2.29)$$

The complete set of positive- and negative-energy free solutions is

$$\psi_{\mathbf{p}\lambda}(t, \mathbf{x}) = N \begin{pmatrix} 1 \\ \frac{\boldsymbol{\sigma} \cdot \mathbf{p}}{\lambda E + m} \end{pmatrix} \mathcal{U} e^{[i(\mathbf{p} \cdot \mathbf{x} - \lambda E t)]}, \quad (2.30)$$

where N is the normalization constant determined from

$$\int d^3x \psi_{\mathbf{p}\lambda}^\dagger(t, \mathbf{x}) \psi_{\mathbf{p}'\lambda'}(t, \mathbf{x}) = \delta_{\lambda\lambda'} \delta(\mathbf{p} - \mathbf{p}'), \quad (2.31)$$

and yielding

$$N = \sqrt{\frac{\lambda E + m}{2\lambda E}}. \quad (2.32)$$

2.4.2 The helicity representation of the Free Dirac Spinor

Helicity is the projection of spin onto the direction of the momentum. It is a quantum number used to classify free one-particle states.

The helicity representation of a free positive-energy Dirac spinor can be written as

$$\mathcal{U}(\mathbf{k}, h) = \left(\frac{E_k + M}{2E_k} \right)^{1/2} \begin{pmatrix} \phi_h(\hat{\mathbf{k}}) \\ \frac{h|\mathbf{k}|}{E_k + M} \phi_h(\hat{\mathbf{k}}) \end{pmatrix}, \quad (2.33)$$

where E_k is the energy of a particle of three momentum \mathbf{k} and the mass M , $\hat{\mathbf{k}}$ is the direction of momentum and $h = \pm 1$ is the helicity. $\phi_h(\hat{\mathbf{k}})$ represents a Pauli-spinor and is defined for an electron propagating in the \mathbf{z} -direction (i.e. $\mathbf{k} = (0, 0, |\mathbf{k}|)$) as

$$\phi_h(\hat{\mathbf{k}}) = \begin{pmatrix} 1 \\ 0 \end{pmatrix} \quad \text{for } h = +1, \quad (2.34)$$

and

$$\phi_h(\hat{\mathbf{k}}) = \begin{pmatrix} 0 \\ 1 \end{pmatrix} \quad \text{for } h = -1. \quad (2.35)$$

For massless particles (i.e., $M = 0$), where $|\mathbf{k}| = E_k$, one can readily derive the following expression

$$\mathcal{U}(\mathbf{k}, h)\bar{\mathcal{U}}(\mathbf{k}, h) = \frac{\not{k}}{4E_k}(I_4 - h\gamma^5), \quad (2.36)$$

where $\not{k} = \gamma_\mu k^\mu$, and I_4 and γ^5 are respectively defined as

$$I_4 = \begin{pmatrix} I_2 & 0 \\ 0 & I_2 \end{pmatrix} \quad \text{and} \quad \gamma^5 = \begin{pmatrix} 0 & I_2 \\ I_2 & 0 \end{pmatrix}. \quad (2.37)$$

2.5 Bound state wavefunction

In this section we use the relativistic mean-field approximation to the Walecka model [39] to obtain an expression of the bound state wave-function for the bound nucleon.

We start by recalling that the Dirac equation with external potentials is given by

$$[\boldsymbol{\alpha} \cdot \mathbf{p} + \beta(m + V_s) + \mathbf{V}_v] \psi = \epsilon \psi, \quad (2.38)$$

where α and β are given by Eq. (2.15) and V_s and \mathbf{V}_v represent scalar and vector potentials respectively.

Considering relativistic mean field theory with spherical symmetry for which the scalar and vector potentials depend only on the radial coordinate, the orbital angular momentum is not a conserved quantum number. Instead the Dirac bound-state spinor of the nucleon moving in a spherical relativistic field can be classified with respect to a generalized angular momentum κ , which represent the eigenvalue of the operator [38, 40, 41]

$$\hat{\kappa} = -\beta(\boldsymbol{\sigma} \cdot \hat{\mathbf{L}} + 1), \quad (2.39)$$

with $\kappa = \pm(j + \frac{1}{2})$, where $(-)$ for aligned spin ($s_{1/2}$, $p_{3/2}$, etc); and $(+)$ for unaligned spin ($p_{1/2}$, $d_{3/2}$, etc). The operator $\hat{\kappa}$ determines, in the non-relativistic limit, whether the

projection of the spin is parallel to the total angular momentum. Thus, the quantum number κ and the projection of the total angular momentum j on the z -axis, m , are sufficient to label the orbitals. These states can be expressed in a two-component representation as:

$$\mathcal{U}_{E\kappa m}(\mathbf{x}) = \frac{1}{x} \begin{pmatrix} g_{E\kappa}(x)\mathcal{Y}_{+\kappa m}(\hat{\mathbf{x}}) \\ if_{E\kappa}(x)\mathcal{Y}_{-\kappa m}(\hat{\mathbf{x}}) \end{pmatrix}, \quad (2.40)$$

where the spin-angular functions are defined as

$$\mathcal{Y}_{\kappa m}(\hat{\mathbf{x}}) \equiv \langle \hat{\mathbf{x}} | \ell \frac{1}{2} j m \rangle; \quad j = |\kappa| - \frac{1}{2}; \quad \ell = \begin{cases} \kappa & \text{if } \kappa > 0 \\ -1 - \kappa & \text{if } \kappa < 0 \end{cases}, \quad (2.41)$$

and $g_{E\kappa}$ and $f_{E\kappa}$ are the upper and lower component of the radial Dirac equation given by [42, 43, 44]

$$\left[\frac{d}{dr} + \frac{1 + \kappa}{r} \right] g_{E\kappa} = [1 + E - V(r)] f_{E\kappa}, \quad (2.42)$$

and

$$\left[\frac{d}{dr} + \frac{1 - \kappa}{r} \right] f_{E\kappa} = [1 - E + V(r)] g_{E\kappa}, \quad (2.43)$$

where E represents the energy of the bound nucleon, and $V(r)$ is the coulomb potential.

Relativistic mean-field models have been successful in describing and predicting properties of finite nuclei. The (QHD-I) model based on baryons and vector and scalar mesons, was introduced in 1974 by Walecka to discuss high-density matter [45]. The model QHD-II, which includes a renormalizable description of the interaction of charged vector (ρ) and pseudoscalar (π) fields was developed later by Serot and applied to finite nuclei [46]. Other models have been successfully developed in recent years providing mean-field descriptions of the properties of medium to heavy nuclei and have enjoyed enormous success. An example of such a successful development is the NL3 parameter set of Lalazissis. In this work we invoke the FSUGold parameter set [47]. This model provide a good agreement with experimental data [48].

The upper $g(r)$ and the lower $f(r)$ radial wave functions in position space are obtained from the FSUGold model for orbitals . As an example the upper and lower components

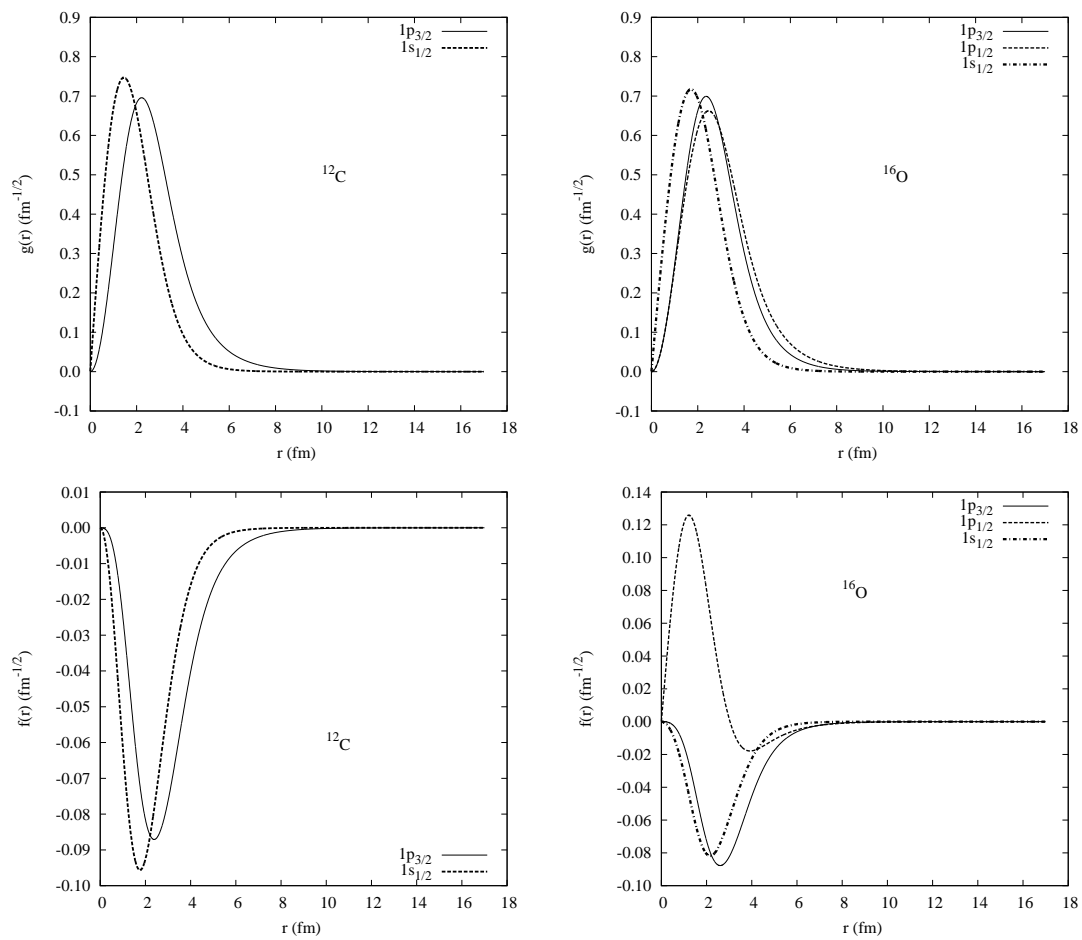


FIG. 2.3. Upper and lower radial wave function $g(r)$ and $f(r)$ for the orbitals $1s_{1/2}$ and $1p_{3/2}$ of ^{12}C and the orbitals $1s_{1/2}$, $1p_{1/2}$ and $1p_{3/2}$ of ^{16}O

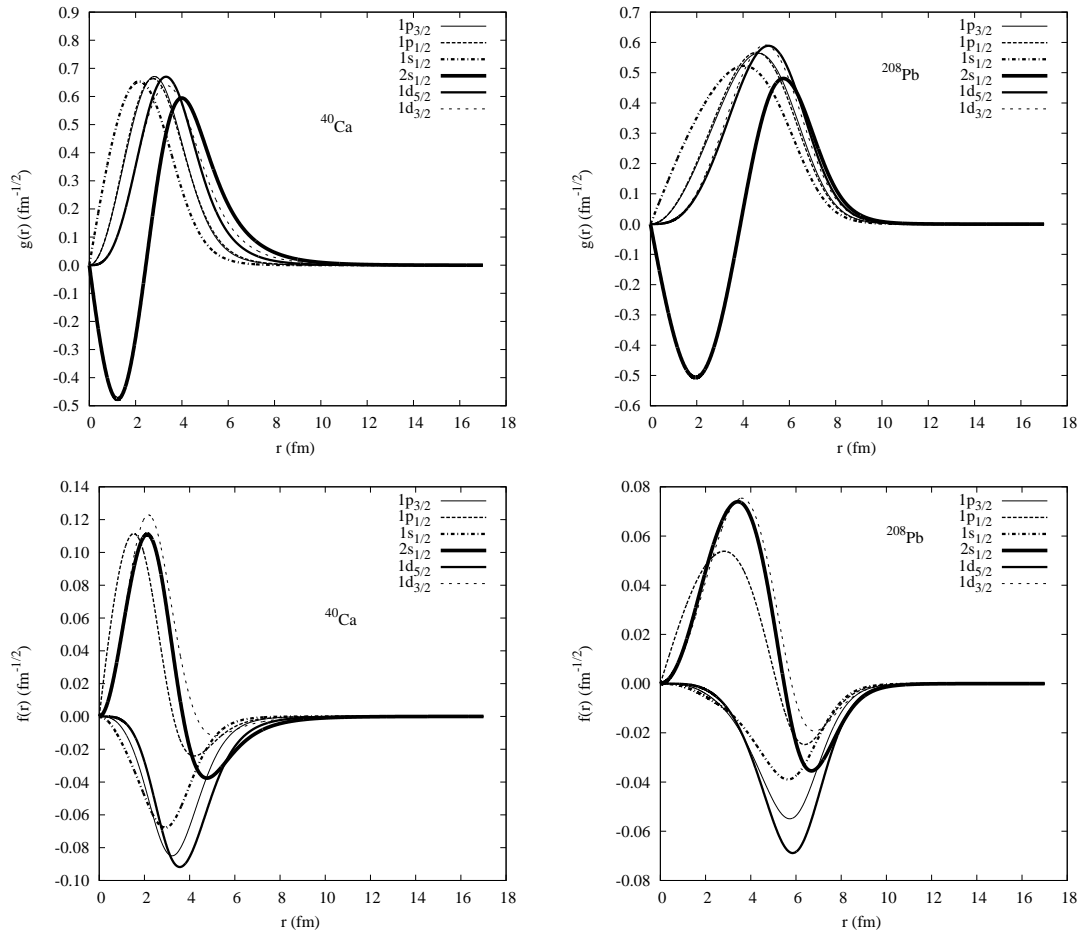


FIG. 2.4. Upper and lower radial wave function $g(r)$ and $f(r)$ for the orbitals $1s_{1/2}$, $2s_{1/2}$, $1p_{3/2}$, $1p_{1/2}$, $1d_{5/2}$, $1d_{3/2}$ of ^{40}Ca and the orbitals $1s_{1/2}$, $2s_{1/2}$, $1p_{3/2}$, $1p_{1/2}$, $1d_{5/2}$, $1d_{3/2}$ of ^{208}Pb

for the $1p_{3/2}$ and $1s_{1/2}$ of the ^{12}C nucleus and for the orbitals $1p_{3/2}$, $1p_{1/2}$ and $1s_{1/2}$ of the ^{16}O nucleus is shown in Fig. 2.3.

We also display the upper and lower radial wave functions in position space for all orbitals of ^{40}Ca and ^{208}Pb , [see Figs. (2.4 - 2.5)]

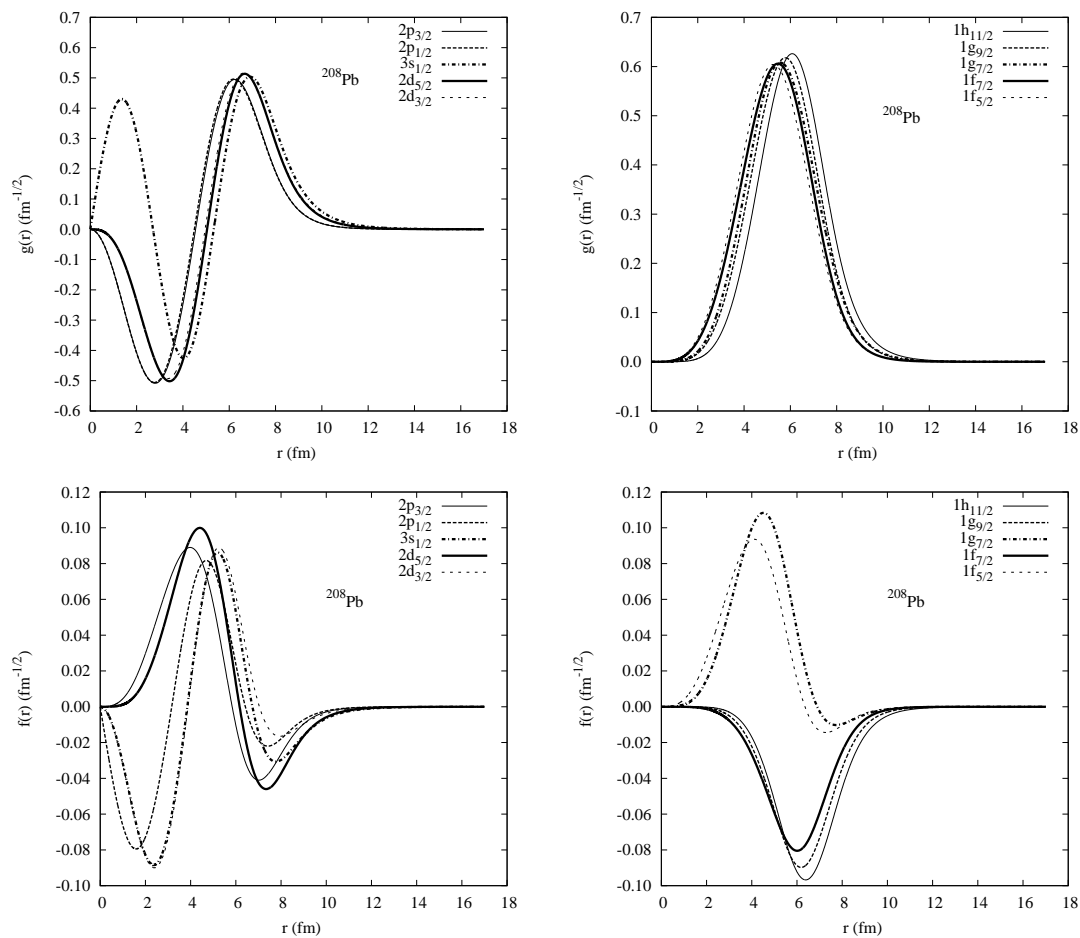


FIG. 2.5. Upper and lower radial wave function $g(r)$ and $f(r)$ for the orbitals $3s_{1/2}$, $2p_{1/2}$, $2p_{3/2}$, $2d_{5/2}$, $2d_{3/2}$ of ^{208}Pb and the orbitals $1h_{11/2}$, $1g_{9/2}$, $1g_{7/2}$, $1f_{7/2}$, $1f_{5/2}$ of ^{208}Pb

Chapter 3

Quasifree Electroproduction of Mesons from Nuclei

In this chapter we present our theoretical model for quasifree meson electroproduction from nuclei. The process we consider in this work can be viewed as the interaction between an incident electron with a bound nucleon via the exchange of a virtual photon. As a result of this interaction, a pseudo-scalar meson (like K , π or η) is produced in association with a nucleon (or an excited state of the nucleon like the lambda hyperon Λ) and some new recoil “daughter” nucleus. Starting with an incident electron on some nucleus, we end up with an outgoing electron, a meson, a free nucleon (or an excited state of it), and a new recoil nucleus. This process is named “quasifree” since the interaction is assumed to take place from only one of the nucleons inside the nucleus. It will be shown that the scattering differential cross section can be written in the form of a contraction between a leptonic and a hadronic tensor. Also the transition current responsible for the meson-electroproduction will be constructed in terms of six invariant amplitudes and six Lorentz- and gauge invariant quantities.

3.1 Schematic picture

The case we are considering in this work is the quasifree electroproduction of the K^+ meson and an unbound Λ -hyperon from nuclei, and it is shown schematically in Fig. 3.1, in which

the basic reaction process is schematically written as

$$e(\mathbf{k}, h) + A(\mathbf{P}) \longrightarrow e(\mathbf{k}', h') + K^+(\mathbf{p}'_1) + \Lambda(\mathbf{p}'_2) + A_{\text{res}}(\mathbf{P}'), \quad (3.1)$$

where A and A_{res} represent the initial and the residual nucleus respectively. Here K^+ is considered to be free and Λ to be an unbound excited state of the nucleon. The recoil nucleus is viewed here as a spectator, i.e, this means that there will be no effect (correction) between the recoil nucleus and the outgoing particles.

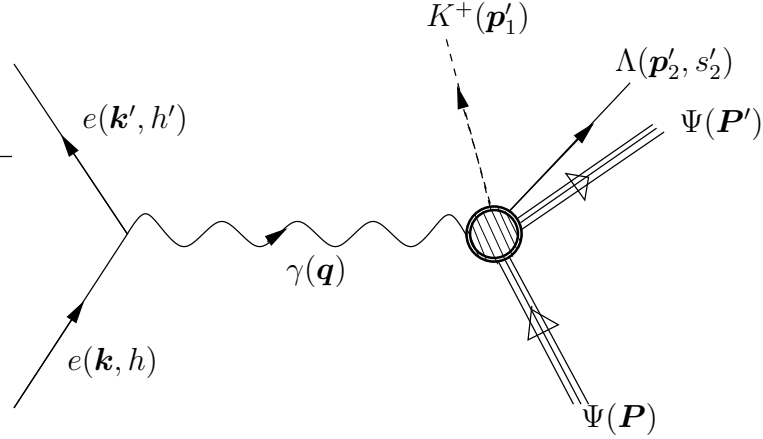


FIG. 3.1. Lowest order Feynman diagram for the electroproduction of mesons and hyperons from nuclei

3.2 Basic ingredients

We assume the extreme relativistic limit, where the electron energy is much larger than the electron mass. We use the helicity representation of the free Dirac spinor, $\mathcal{U}(\mathbf{k}, h)$, [see Sec. 2.4.2]. In the laboratory frame, the four-momentum of the incoming electron is $k = (E_k, \mathbf{k})$, and the outgoing electron four-momentum is $k' = (E_{k'}, \mathbf{k}')$. The virtual photon exchanged between the incident electron and the target nucleus has a four-momentum $q = k - k' = (\omega, \mathbf{q})$. The produced K^+ -meson and Λ -hyperon have four momenta of $p'_1 = (E_{p'_1}, \mathbf{p}'_1)$ and $p'_2 = (E_{p'_2}, \mathbf{p}'_2)$, respectively. The target nucleus is at rest, hence the four momentum is $P = (M, 0)$ and the recoiling residual nucleus has mass of M' with three-momentum $\mathbf{P}' = \mathbf{q} - \mathbf{p}'_1 - \mathbf{p}'_2$. We employ the relativistic plane wave impulse approximation, where we neglect distortion effects on the produced meson and the outgoing hyperon.

3.3 Cross section for pseudoscalar-meson electroproduction

Let us consider the electromagnetic production of a pseudoscalar K^+ meson and a free Λ -hyperon [see Eq. (3.1)] as illustrated in Fig. 3.1. In order to derive the differential cross section for this process, we need to make some assumptions for our model. We define the position space representation $\phi(x) = N_V e^{-ip \cdot x}$ for the free spin-0 particles, and $\psi(x) = N_V \mathcal{U}(\mathbf{p}, s) e^{-ip \cdot x}$ for the spin- $\frac{1}{2}$ particles, where N_V is the normalization constant that is concerned with the particle density and has nothing to do with spinor normalization. In order to take in account both massless and massive particles, we normalize the spinor as follows

$$\mathcal{U}^\dagger \mathcal{U} = 1.$$

Using Fermi's golden rule the differential cross section can be written as [3, 11, 49]

$$d\sigma = \frac{(2\pi)^4 \delta^4(k + P - k' - p'_1 - p'_2 - P')}{|\mathbf{v}_1 - \mathbf{v}_2|} \frac{d^3 \mathbf{k}'}{(2\pi)^3} \frac{d^3 \mathbf{p}'_1}{2E_{p'_1}} \frac{d^3 \mathbf{p}'_2}{(2\pi)^3} \frac{d^3 \mathbf{P}'}{(2\pi)^3} |\mathcal{M}|^2 \quad (3.2)$$

where $|\mathbf{v}_1 - \mathbf{v}_2|$ is the relative initial velocity. In the extreme relativistic limit where the electron mass can be neglected with respect to the electron energy, the initial flux in the laboratory frame is equal to one. Then we can rewrite the Eq. (3.2) as:

$$d\sigma = \frac{1}{(2\pi)^8} d^3 \mathbf{k}' \frac{d^3 \mathbf{p}'_1}{2E_{p'_1}} d^3 \mathbf{p}'_2 d^3 \mathbf{P}' \delta^4(k + P - k' - p'_1 - p'_2 - P') |\mathcal{M}|^2. \quad (3.3)$$

The spatial part of the four-dimensional Dirac δ -function allows the integral over $d^3 \mathbf{P}'$ to be performed. This fixes the three-momentum of the recoil nucleus to be

$$\mathbf{P}' = \mathbf{k} - \mathbf{k}' - \mathbf{p}'_1 - \mathbf{p}'_2 = \mathbf{q} - \mathbf{p}'_1 - \mathbf{p}'_2, \quad (3.4)$$

where $\mathbf{q} = \mathbf{k} - \mathbf{k}'$ is the three momentum transfer to the target nucleus. Hence the differential cross-section Eq. (3.3) becomes:

$$d\sigma = \frac{1}{(2\pi)^8} d^3 \mathbf{k}' \frac{d^3 \mathbf{p}'_1}{2E_{p'_1}} d^3 \mathbf{p}'_2 \delta(E_k + M - E_{k'} - E_{p'_1} - E_{p'_2} - E_{P'}) |\mathcal{M}|^2. \quad (3.5)$$

Now using the geometry of the process, we can write :

$$d^3 \mathbf{k}' = (E_{k'}^2 - m_e^2)^{1/2} E_{k'} dE_{k'} d\Omega_{k'} = 2\pi E_{k'}^2 dE_{k'} d(\cos \theta_e) \quad (3.6a)$$

$$d^3 \mathbf{p}'_1 = (E_{p'_1}^2 - M_{K^+}^2)^{1/2} E_{p'_1} dE_{p'_1} d\Omega_{p'_1} \quad (3.6b)$$

$$d^3 \mathbf{p}'_2 = (E_{p'_2}^2 - M_\Lambda^2)^{1/2} E_{p'_2} dE_{p'_2} d\Omega_{p'_2}. \quad (3.6c)$$

In Appendix A it is shown that the differential cross section for the electromagnetic production of a meson and a hyperon from the electron-nucleus laboratory-frame can be written as

$$\frac{d^5\sigma}{dE_{k'} d(\cos\theta_e) dE_{p'_1} d\Omega_{p'_1} d\Omega_{p'_2}} = \mathcal{K} |\mathcal{M}|^2, \quad (3.7)$$

where \mathcal{K} is the kinematic quantity given in Eq. (3.17), that is fully determined by the energies and masses of the reaction particles, as well as the scattering angles of the ejected particles.

3.4 The kinematics

Let us now discuss the kinematics for the production of an unbound nucleon from a nucleus. We assume quasifree kinematics, i.e., the electron interacts with only one bound proton. This is depicted in Fig. 3.2,

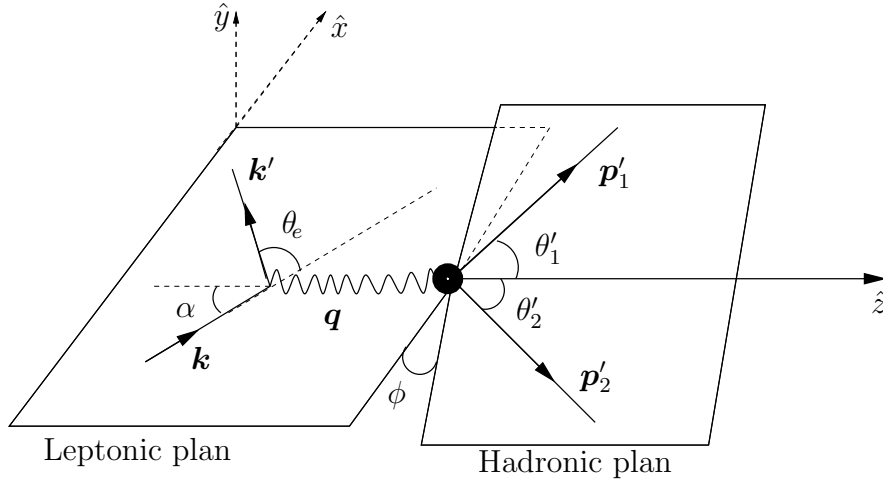


FIG. 3.2. The coordinate system of the reaction $A(e, e' K^+ \Lambda)A_{\text{RES}}$ in the laboratory frame .

where the direction of the virtual photon three-momentum \mathbf{q} defines the \hat{z} axis, as:

$$\hat{z} = \frac{\mathbf{q}}{|\mathbf{q}|}. \quad (3.8)$$

The leptonic plane is defined by the unit vectors $\hat{\mathbf{x}}$ and $\hat{\mathbf{z}}$, and the right-handed coordinate system completed by defining

$$\hat{\mathbf{y}} = \hat{\mathbf{x}} \times \hat{\mathbf{z}}. \quad (3.9)$$

The direction of the incident electron beam with respect to the z -axis is defined by the angle α , while the electron scattering angle is θ_e . The hadronic plane makes an angle ϕ with respect to the leptonic plane. The K^+ and unbound Λ particles scatter in the hadronic plane with angles θ'_1 and θ'_2 with respect to the z -axis. Next we derive expressions that fully specify the following four-vectors in the laboratory frame:

$$\begin{aligned} q^\mu &= (\omega, 0, 0, q_z) \\ k^\mu &= (E_k, k_x, 0, k_z) \\ k'^\mu &= (E_{k'}, k'_x, 0, k'_z) \\ p_1'^\mu &= (E_{p'_1}, p'_{1x}, p'_{1y}, p'_{1z}) \\ p_2'^\mu &= (E_{p'_2}, p'_{2x}, p'_{2y}, p'_{2z}). \end{aligned} \quad (3.10)$$

Assuming massless electrons, the magnitude of the three momenta of the incident and outgoing electron in the laboratory frame are given by:

$$|\mathbf{k}| = E_k \quad \text{and} \quad |\mathbf{k}'| = E_{k'}. \quad (3.11)$$

From Fig. 3.2 we also have that

$$\mathbf{k} = (E_k, \mathbf{k}) = E_k (1, \sin \alpha, 0, \cos \alpha) \quad (3.12)$$

$$\mathbf{k}' = (E_{k'}, \mathbf{k}') = E_{k'} (1, \sin(\alpha + \theta_e), 0, \cos(\alpha + \theta_e)). \quad (3.13)$$

In addition, we require that the virtual photon moves only following the z -axis, such that the three-momentum (or the three-momentum transfer) will only have a z -component, and the angle α is given by

$$\sin \alpha = \pm \left[\frac{E_{k'}^2 \sin^2 \theta_e}{E_k^2 + E_{k'}^2 - 2E_k E_{k'} \cos \theta_e} \right]^{1/2}. \quad (3.14)$$

Geometric arguments from Fig. 3.2 can be used to determine the four-vectors momentum of the K^+ -meson and the outgoing nucleon. In the laboratory frame, for the K^+ -meson we have that

$$\mathbf{p}'_1 = |\mathbf{p}'_1| \sin \theta'_1 \cos \phi \hat{\mathbf{x}} + |\mathbf{p}'_1| \sin \theta'_1 \sin \phi \hat{\mathbf{y}} + |\mathbf{p}'_1| \cos \theta'_1 \hat{\mathbf{z}} \quad (3.15)$$

where $|\mathbf{p}'_1| = \sqrt{E_{p'_1}^2 - M_{K^+}^2}$. The three-momentum of the hyperon is given by

$$\mathbf{p}'_2 = |\mathbf{p}'_2| \sin \theta'_2 \cos \phi \hat{\mathbf{x}} + |\mathbf{p}'_2| \sin \theta'_2 \sin \phi \hat{\mathbf{y}} + |\mathbf{p}'_2| \cos \theta'_2 \hat{\mathbf{z}} \quad (3.16)$$

with $|\mathbf{p}'_2| = \sqrt{E_{p'_2}^2 - m_\Lambda^2}$. Finally we find the following expression for the kinematics factor

$$\mathcal{K} = \frac{E_{k'}^2}{(2\pi)^7} (E_{p'_1}^2 - M_{K^+}^2)^{1/2} (E_{p'_2}^2 - M_\Lambda^2)^{1/2} \delta[f(E_{p'_2})] dE_{p'_2}, \quad (3.17)$$

where $f(E_{p'_2})$ is the function given in Eq. (A.29), [See Appendix A]. Thus far we have only considered kinematics. Next we focus on dynamical aspects underlying the interaction process.

3.5 Dynamics of the process

All dynamical information concerning the scattering process is contained in the transition matrix element \mathcal{M} which is defined as:

$$\mathcal{M} = [\bar{\mathcal{U}}(\mathbf{k}', h') \gamma_\mu \mathcal{U}(\mathbf{k}, h)] \left(\frac{e^2}{q^2} \right) \langle \mathbf{p}'_1; \mathbf{p}'_2, s'_2; \Psi_f(\mathbf{P}') | \hat{J}^\mu(q) | \Psi_i(\mathbf{P}) \rangle, \quad (3.18)$$

where h and h' are the helicity states for spin parallel or anti-parallel to the direction of the momentum. In Eq. (3.18) \hat{J}^μ is the hadronic current operator, and $\mathcal{U}(\mathbf{k}, h)$ and $\mathcal{U}(\mathbf{k}', h')$ are respectively the plane wave Dirac spinor for the incident and ejectile electrons. $|\Psi_i(\mathbf{P})\rangle$ represents the many-body state for the target nucleus, and $|\mathbf{p}'_1; \mathbf{p}'_2, s'_2; \Psi_f(\mathbf{P}')\rangle$ represents the final state consisting of many-body residual nucleus state, outgoing meson and hyperon.

Using Eq. (3.18) it follows that

$$|\mathcal{M}|^2 = \mathcal{M} \mathcal{M}^* = \left(\frac{e^2}{q^2} \right)^2 L_{\mu\nu} W^{\mu\nu}, \quad (3.19)$$

where we have introduced the leptonic tensor

$$L_{\mu\nu} = \sum_{h, h' = \pm 1} [\bar{\mathcal{U}}(\mathbf{k}', h') \gamma_\mu \mathcal{U}(\mathbf{k}, h)] [\bar{\mathcal{U}}(\mathbf{k}', h') \gamma_\nu \mathcal{U}(\mathbf{k}, h)]^*, \quad (3.20)$$

and the hadronic tensor

$$W^{\mu\nu} = \sum_{s'_2} \left[\langle \mathbf{p}'_1; \mathbf{p}'_2, s'_2; \Psi_f(\mathbf{P}') | \hat{J}^\mu(q) | \Psi_i(\mathbf{P}) \rangle \right] \left[\langle \mathbf{p}'_1; \mathbf{p}'_2, s'_2; \Psi_f(\mathbf{P}') | \hat{J}^\nu(q) | \Psi_i(\mathbf{P}) \rangle \right]^*. \quad (3.21)$$

3.5.1 Leptonic tensor

Using the helicity representation of the free Dirac spinor, the leptonic tensor is given by

$$L_{\mu\nu} = \sum_{h,h'=\pm 1} [\bar{\mathcal{U}}(\mathbf{k}', h') \gamma_\mu \mathcal{U}(\mathbf{k}, h)] [\bar{\mathcal{U}}(\mathbf{k}', h') \gamma_\nu \mathcal{U}(\mathbf{k}, h)]^*, \quad (3.22)$$

where

$$\mathcal{U}(\mathbf{k}, h) = \left(\frac{E_k + M}{2E_k} \right)^{1/2} \begin{pmatrix} \phi_h(\hat{\mathbf{k}}) \\ \frac{h|\mathbf{k}|}{E_k + M} \phi_h(\hat{\mathbf{k}}) \end{pmatrix} \quad (3.23)$$

For the massless leptons we have that

$$\mathcal{U}(\mathbf{k}, h) = \frac{1}{\sqrt{2}} \begin{pmatrix} \phi_h(\hat{\mathbf{k}}) \\ h\phi_h(\hat{\mathbf{k}}) \end{pmatrix} \quad (3.24)$$

where the matrix $\phi_h(\hat{\mathbf{k}})$ is given by

$$\phi_h(\hat{\mathbf{k}}) = \begin{pmatrix} (\cos \frac{\theta}{2})\delta_{h,1} - e^{-i\phi}(\sin \frac{\theta}{2})\delta_{h,-1} \\ e^{i\phi}(\sin \frac{\theta}{2})\delta_{h,1} + (\cos \frac{\theta}{2})\delta_{h,-1} \end{pmatrix}. \quad (3.25)$$

Using Eqs. (3.24)-(3.25), we obtain the following identity

$$\mathcal{U}(\mathbf{k}, h)\bar{\mathcal{U}}(\mathbf{k}, h) = \frac{1}{4E} \not{k}[(I_4 - h\gamma^5)]. \quad (3.26)$$

According to the helicity dependence of the incoming and outgoing leptons, four cases for the leptonic tensor may be considered:

- unpolarized incident and outgoing leptonic beams [Eq. (3.27a)]
- polarized incident and unpolarized outgoing leptonic beams [Eq. (3.27b)]
- unpolarized incident and polarized outgoing leptonic beams [Eq. (3.27c)]
- polarized incident and outgoing leptonic beams [Eq. (3.27d)]

$$L_{\mu\nu}^{(0)}(k; k') = \frac{1}{E_k E_{k'}} [k_\mu k'_\nu + k'_\mu k_\nu - k \cdot k' g_{\mu\nu}] \quad (3.27a)$$

$$L_{\mu\nu}^{(1)}(k, h; k') = \frac{1}{2E_k E_{k'}} [k_\mu k'_\nu + k'_\mu k_\nu - g_{\mu\nu} k \cdot k' - i h k^\alpha k'^\beta \epsilon_{\mu\nu\alpha\beta}] \quad (3.27b)$$

$$L_{\mu\nu}^{(2)}(k; k', h') = \sum_{h=\pm 1} L_{\mu\nu} = L_{\mu\nu}^{(1)}(k', h'; k) \quad (3.27c)$$

$$L_{\mu\nu}(k, h; k', h') = \frac{1}{4E_k E_{k'}} \left[(1 + h h') (k_\mu k'_\nu + k'_\mu k_\nu - k \cdot k' g_{\mu\nu}) - i (h + h') k^\alpha k'^\beta \epsilon_{\mu\nu\alpha\beta} \right], \quad (3.27d)$$

The derivation of the above expressions is done in appendix B. One can use those expression to verify the preservation of the helicity.

3.5.2 Hadronic tensor

The hadronic tensor is given by

$$W^{\mu\nu} = \sum_{s'_2} \left[\langle p'_1; p'_2, s'_2; \Psi_f(P') | \hat{J}^\mu(q) | \Psi_i(P) \rangle \right] \left[\langle p'_1; p'_2, s'_2; \Psi_f(P') | \hat{J}^\nu(q) | \Psi_i(P) \rangle \right]^*. \quad (3.28)$$

The hadronic matrix element can be written as

$$J^\mu = \sum_{s'_2} \langle p'_1; p'_2, s'_2; \Psi_f(P') | \hat{J}^\mu(q) | \Psi_i(P) \rangle, \quad (3.29)$$

where $\hat{J}^\mu(q)$ is the transition current of the process.

The general structure of the transition current for the K^+ -meson and the unbound Λ electromagnetic production is dictated by Lorentz- and gauge invariant quantities, and this is a very complicated quantity to deal with. The approximation illustrated in Fig. 3.3 shows that hadronic current of the electromagnetic production process of mesons and hyperons can be determined from the elementary process

$$\gamma(\text{virtual}) + \text{nucleon} \longrightarrow \text{meson} + \text{hyperon}. \quad (3.30)$$

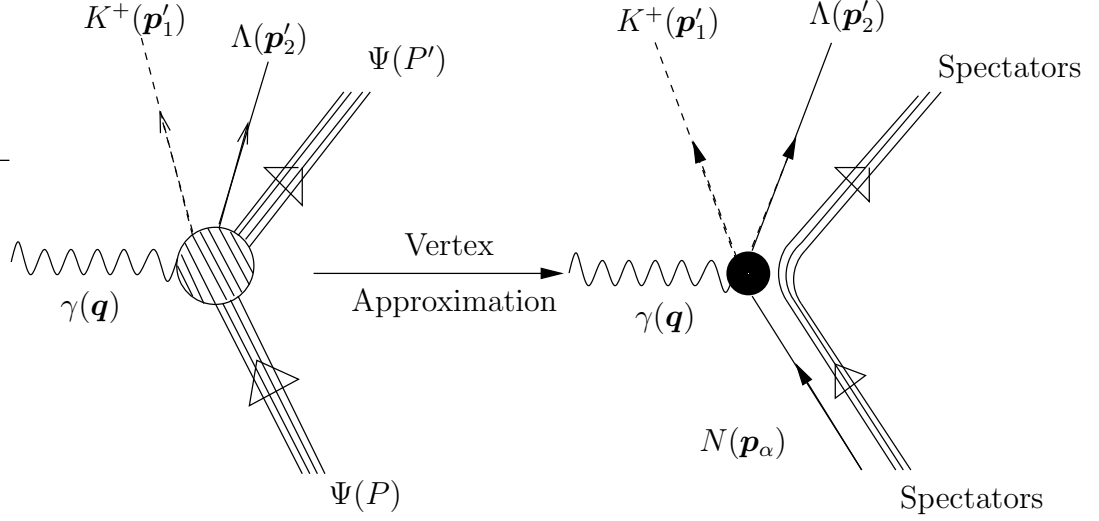


FIG. 3.3. Approximation employed at the hadronic vertex in order to obtain a tractable form of the matrix element for the electromagnetic production of meson and unbound hyperon from the single bound nucleon.

In general there are six reaction channels which may be explored using this formalism, namely

$$e + p \longrightarrow e + K^+ + \Lambda \quad (3.31a)$$

$$e + n \longrightarrow e + K^0 + \Lambda \quad (3.31b)$$

$$e + p \longrightarrow e + K^+ + \Sigma^0 \quad (3.31c)$$

$$e + n \longrightarrow e + K^0 + \Sigma^0 \quad (3.31d)$$

$$e + p \longrightarrow e + K^0 + \Sigma^+ \quad (3.31e)$$

$$e + n \longrightarrow e + K^+ + \Sigma^- . \quad (3.31f)$$

Our developed formalism will only consider the case for the electroproduction of hyperons. We make a number of assumptions for the hadronic vertex. We first assume that only one single bound proton couples to the photon emitted by the scattering electron. Here, we neglect two- and many-body corrections to the hadronic current operator. As a second assumption, we neglect two- and many- body rescattering processes in the final channel. We also neglect all nuclear distortion effects on the produced kaon and hyperon, so that they can be treated as free particles. All these simplifying assumptions and approximations enable us to express the hadronic current operator in the following form

$$J^\mu = \sum_{m, s'_2} \bar{U}(\mathbf{p}'_2, s'_2) \hat{J}^\mu(q) U_{\alpha, m}(\mathbf{p}_m), \quad (3.32)$$

where α denotes the collection of quantum numbers associated with a particular bound nucleon coupled to the photon, and $\hat{J}^\mu(q)$ represents the hadronic current operator.

The hadronic current operator for the electroproduction of hyperons can be written as a linear combination of six invariant amplitudes and six Lorentz- and gauge invariant quantities as follows [2, 50, 49]

$$\hat{J}^\mu = \sum_{i=1}^6 A_i(s, t, q^2) \mathcal{M}_i^\mu, \quad (3.33)$$

where s and t represent Mandelstam variables defined as

$$s = (q + p)^2 = (p'_1 + p'_2)^2 \quad (3.34a)$$

$$t = (q - p'_1)^2 = (p'_2 - p)^2 \quad (3.34b)$$

$$u = (q - p'_2)^2 = (p'_1 - p)^2. \quad (3.34c)$$

The six Lorentz- and gauge invariant quantities \mathcal{M}_i^μ are given by

$$\mathcal{M}_1^\mu = \frac{1}{2} \gamma^5 (\gamma^\mu \not{q} - \not{q} \gamma^\mu) \quad (3.35a)$$

$$\mathcal{M}_2^\mu = \frac{1}{2} \gamma^5 [(p \cdot q + p'_2 \cdot q)(2p'_1{}^\mu - q^\mu) - (2p'_1 \cdot q - q^2)(p^\mu + p'_2{}^\mu)] \quad (3.35b)$$

$$\mathcal{M}_3^\mu = \gamma^5 (p'_1 \cdot q \gamma^\mu - p'_1{}^\mu \cdot \not{q}) \quad (3.35c)$$

$$\mathcal{M}_4^\mu = -i \epsilon_{\alpha\lambda\beta\nu} p_1'^\beta q^\nu \gamma^\alpha g^{\mu\lambda} \quad (3.35d)$$

$$\mathcal{M}_5^\mu = \gamma^5 (p_1'^\mu q^2 - p'_1 \cdot q q^\mu) \quad (3.35e)$$

$$\mathcal{M}_6^\mu = \gamma^5 (q^\mu \not{q} - q^2 \gamma^\mu) \quad (3.35f)$$

The bound nucleon four-momentum is denoted by p and defined using the approximation made in the hadronic vertex in accordance with momentum conservation:

$$p = p'_1 + p'_2 - q. \quad (3.36)$$

3.6 Nuclear Structure

The relativistic mean field approximation to the Walecka model [39] is used to determine the nuclear structure for the bound state function of the bound nucleon. As we have seen

in Sec. 2.5 the Dirac bound-state spinor of the nucleon moving in a spherical relativistic field can be classified with respect to a generalized angular momentum κ , the eigenstates of the Dirac equation can be expressed in a two component representation as:

$$\mathcal{U}_{E\kappa m}(\mathbf{x}) = \frac{1}{x} \begin{pmatrix} g_{E\kappa}(x) \mathcal{Y}_{+\kappa m}(\hat{\mathbf{x}}) \\ i f_{E\kappa}(x) \mathcal{Y}_{-\kappa m}(\hat{\mathbf{x}}) \end{pmatrix}, \quad (3.37)$$

where the spin-angular functions are defined as

$$\mathcal{Y}_{\kappa m}(\hat{\mathbf{x}}) \equiv \langle \hat{\mathbf{x}} | \ell \frac{1}{2} j m \rangle; \quad j = |\kappa| - \frac{1}{2}; \quad \ell = \begin{cases} \kappa, & \text{if } \kappa > 0 \\ -1 - \kappa, & \text{if } \kappa < 0 \end{cases}. \quad (3.38)$$

Since the scattering matrix element is proportional to the bound-nucleon wave function in momentum space, it is instructive to examine the momentum content of the wave function. The Fourier transform of the relativistic bound-state spinor, allowing the transformation from the spatial representation to the momentum representation, can be written as:

$$\begin{aligned} \mathcal{U}_{E\kappa m}(\mathbf{p}) &\equiv \int d\mathbf{x} e^{-i\mathbf{p}\cdot\mathbf{x}} \mathcal{U}_{E\kappa m}(\mathbf{x}) \\ &= \frac{4\pi}{p} (-i)^\ell \begin{pmatrix} g_{E\kappa}(p) \\ f_{E\kappa}(p) (\vec{\sigma} \cdot \hat{\mathbf{p}}) \end{pmatrix} \mathcal{Y}_{+\kappa m}(\hat{\mathbf{p}}), \end{aligned} \quad (3.39)$$

where the Fourier transforms of the radial wave functions are given by

$$g_{E\kappa}(p) = \int_0^\infty dx g_{E\kappa}(x) \hat{j}_\ell(px), \quad (3.40)$$

and

$$f_{E\kappa}(p) = (\text{sign}\kappa) \int_0^\infty dx f_{E\kappa}(x) \hat{j}_{\ell'}(px). \quad (3.41)$$

In the above expression we have incorporated the Riccati-Bessel function in terms of the spherical Bessel function $\hat{j}_\ell(z) = z j_\ell(z)$ and ℓ' being the orbital angular momentum corresponding to $-\kappa$. We employ in this work the FSUGold model parameter set [47] to determine the momentum space wave function using the Eq. (3.40) and Eq. (3.41). The results for the upper $g(p)$ and the lower $f(p)$ for the proton orbitals as function of momentum are displayed in Fig. 3.4 and Fig. 3.6 for ^{12}C , ^{16}O , ^{40}Ca and ^{208}Pb . In all these figures we can evidently see that most of the wave-functions have the maximum approximately around 100 MeV and they only be appreciable in the range of momentum $p \leq 300$ MeV.

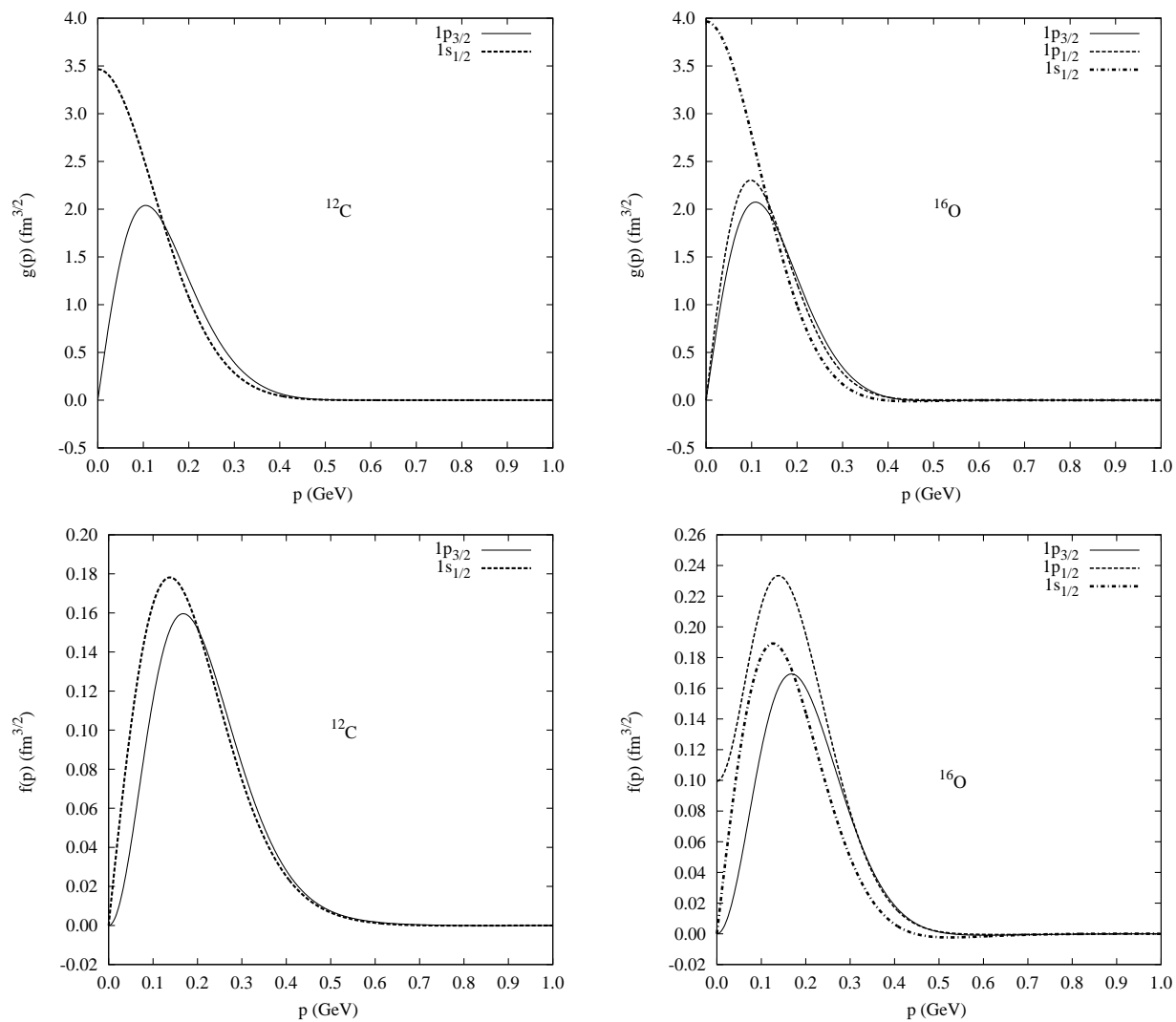


FIG. 3.4. Upper $g(p)$ and lower $f(p)$ component of the radial bound state wave-function of the bound nucleon in the momentum space representation for the orbitals $1s_{1/2}$ and $1p_{3/2}$ of ^{12}C and $1s_{1/2}$, $1p_{1/2}$ and $1p_{3/2}$ of ^{16}O

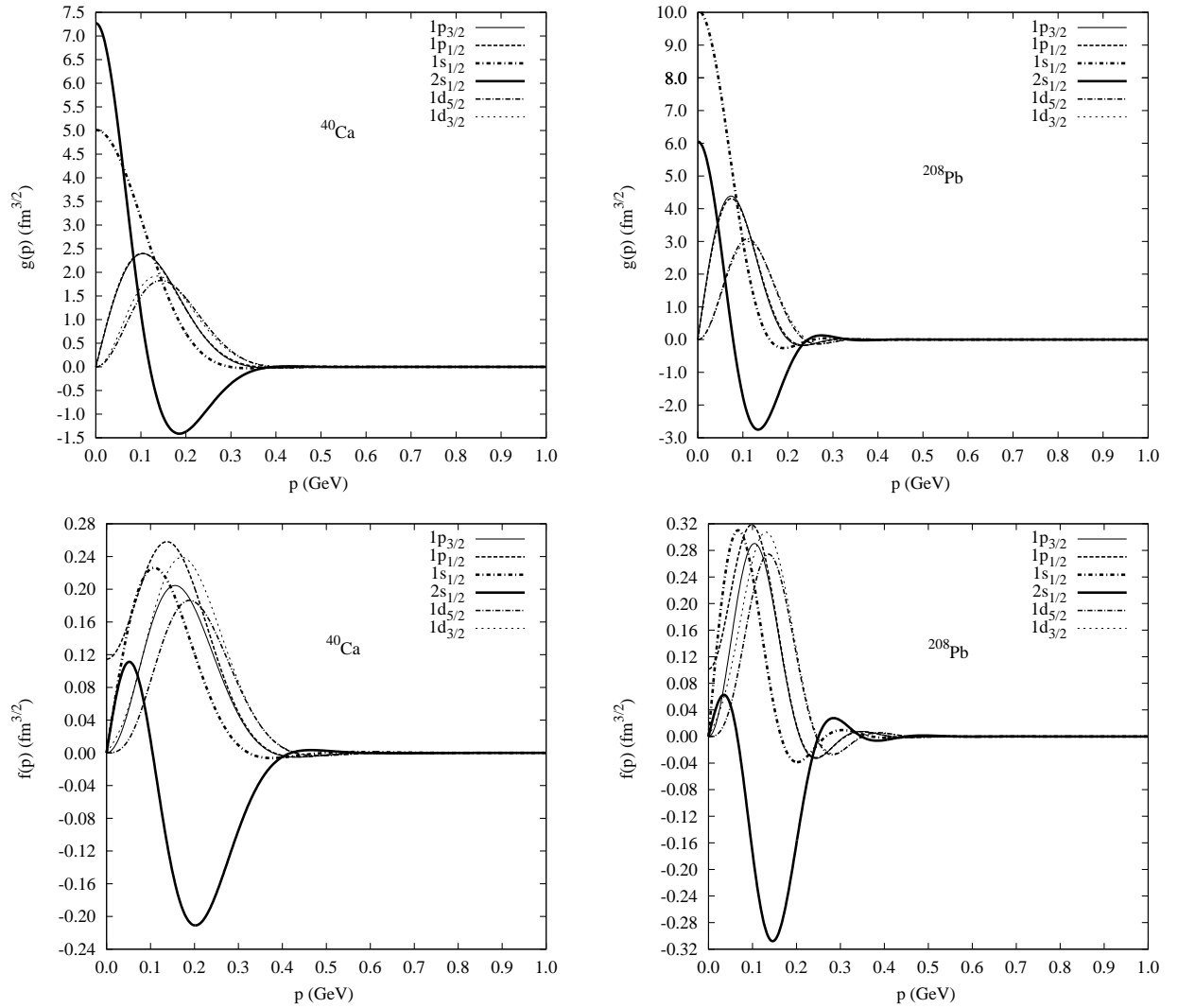


FIG. 3.5. Upper $g(p)$ and lower $f(p)$ component of the radial bound state wave-function of the bound nucleon in the momentum space representation for the orbitals $1s_{1/2}$, $2s_{1/2}$, $1p_{3/2}$, $1p_{1/2}$, $1d_{5/2}$, $1d_{3/2}$ of ^{40}Ca and $1s_{1/2}$, $2s_{1/2}$, $1p_{3/2}$, $1p_{1/2}$, $1d_{5/2}$, $1d_{3/2}$ of ^{208}Pb

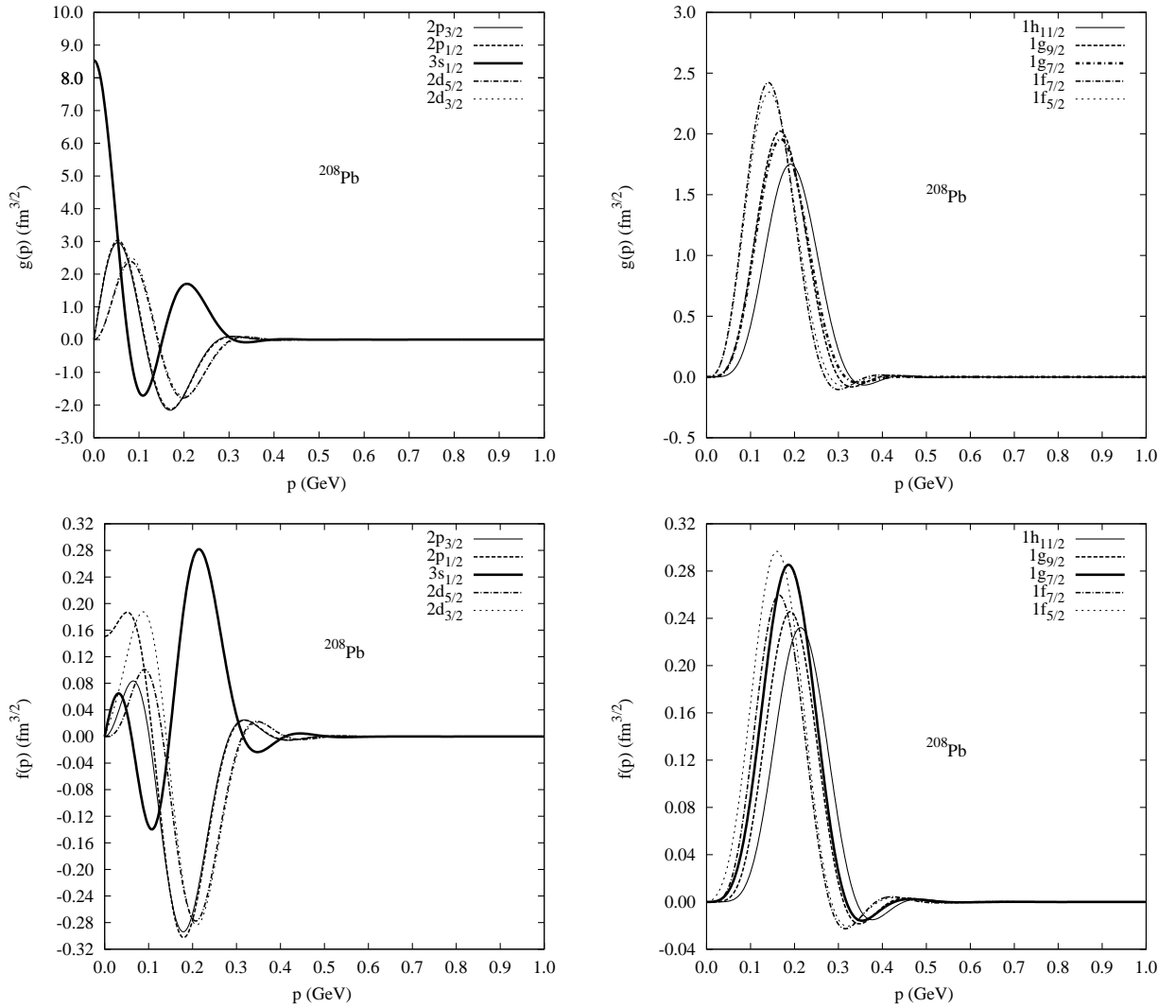


FIG. 3.6. Upper $g(p)$ and lower $f(p)$ component of the radial bound state wave-function of the bound nucleon in the momentum space representation for the orbitals $3s_{1/2}$, $2p_{1/2}$, $2p_{3/2}$, $2d_{5/2}$, $2d_{3/2}$ of ^{208}Pb and $1h_{11/2}$, $1g_{9/2}$, $1g_{7/2}$, $1f_{7/2}$, $1f_{5/2}$ of ^{208}Pb

3.7 Bound State Propagator

Next we find an expression for the bound state propagator of the bound nucleon. We start by invoking the algebraic “trick” introduced for the first time by Casimir [51], which allows one to express the spin projector of the free particle in terms of Dirac gamma matrices as

$$S(p') \equiv \sum_{s'} \mathcal{U}(\mathbf{p}', s') \bar{\mathcal{U}}(\mathbf{p}', s') = \frac{\not{p}' + M'}{2E_{p'}}, \quad (3.42)$$

where M' is the mass of the free particle and its energy is defined as

$$p'^0 \equiv E_{p'} = \sqrt{\mathbf{p}'^2 + M'^2}. \quad (3.43)$$

This trick is very useful because it allows one to use the trace algebra techniques developed by Feynman to compute free polarization observables. Secondly we invoke the useful trick introduced by Gardner and Piekarewicz [52], which shows a similarity of the spin projector of the bound state with the spin projector of the free particle. The spin projector of the bound nucleon can be written in terms of Dirac gamma matrices, using the identities

$$\sum_m \mathcal{Y}_{\pm\kappa m}(\hat{\mathbf{p}}) \mathcal{Y}_{\pm\kappa m}^*(\hat{\mathbf{p}}) = \pm \frac{2j+1}{8\pi} \begin{cases} 1 \\ \boldsymbol{\sigma} \cdot \hat{\mathbf{p}} \end{cases}, \quad (3.44)$$

which enable us to introduce the concept of a bound state propagator, expressed as:

$$\begin{aligned} S_\alpha(\mathbf{p}) &= \frac{1}{2j+1} \sum_m \mathcal{U}_{\alpha,m}(\mathbf{p}) \bar{\mathcal{U}}_{\alpha,m}(\mathbf{p}) \\ &= \left(\frac{2\pi}{p^2} \right) \begin{pmatrix} g_\alpha^2(p) & -g_\alpha(p) f_\alpha(p) \boldsymbol{\sigma} \cdot \hat{\mathbf{p}} \\ g_\alpha(p) f_\alpha(p) \boldsymbol{\sigma} \cdot \hat{\mathbf{p}} & -f_\alpha^2(p) \end{pmatrix} \\ &= (\not{p}_\alpha + M_\alpha); \quad (\alpha = \{E, \kappa\}). \end{aligned} \quad (3.45)$$

In the above equations, $g_\alpha(p)$ and $f_\alpha(p)$ are the Fourier transforms of the upper and lower components of the bound-state Dirac spinor respectively [see Eq. (3.40) and Eq. (3.41)]. We have also defined the mass-, energy- and momentum-like quantities as

$$M_\alpha = \left(\frac{\pi}{p^2} \right) [g_\alpha^2(p) - f_\alpha^2(p)], \quad (3.46a)$$

$$E_\alpha = \left(\frac{\pi}{p^2} \right) [g_\alpha^2(p) + f_\alpha^2(p)], \quad (3.46b)$$

$$\mathbf{p}_\alpha = \left(\frac{\pi}{p^2} \right) [2g_\alpha(p) f_\alpha(p) \hat{\mathbf{p}}], \quad (3.46c)$$

which satisfy the "on-shell relation"

$$p_\alpha^2 = E_\alpha^2 - \mathbf{p}_\alpha^2 = M_\alpha^2, \quad (3.47)$$

where p expresses the missing-momentum and it defined as the magnitude of the bound nucleon three momentum, which will be given by momentum conservation using our approximation at the hadronic vertex. We have examined the behaviour of the mass-, energy- and momentum-like quantities: M_α , E_α and $|\mathbf{p}_\alpha|$. In Fig. 3.7 we present the variables $M_\alpha \times p^2$, $E_\alpha \times p^2$ and $|\mathbf{p}_\alpha| \times p^2$ as function of momentum, while in Fig. 3.8 we display the variables M_α , E_α and $|\mathbf{p}_\alpha|$. Note that here we only use the orbital $1p_{3/2}$ in a ^{12}C nucleus. The radial component of the wave function of the bound-nucleon (proton in our case) in momentum space for this orbital is plotted in Fig. 3.9. Next we determine an expression

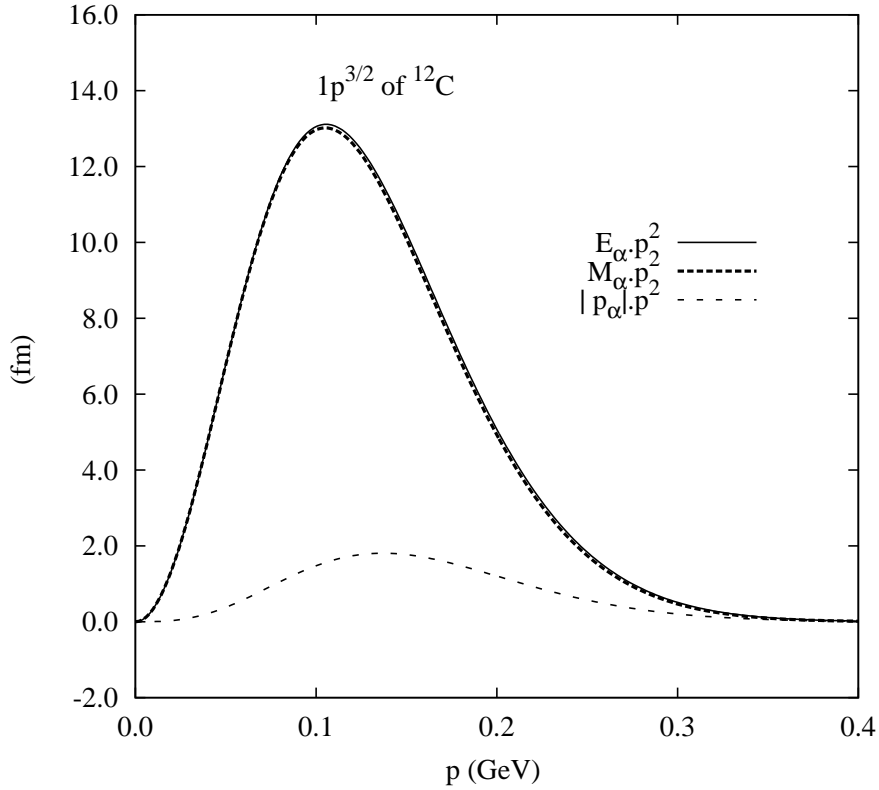


FIG. 3.7. The effective mass-, energy, and momentum-like quantities: M_α , E_α and \mathbf{p}_α as a function of the momentum (p)

for the free hyperon wave function. Since it is a spin- $\frac{1}{2}$ particle, it must be described by a

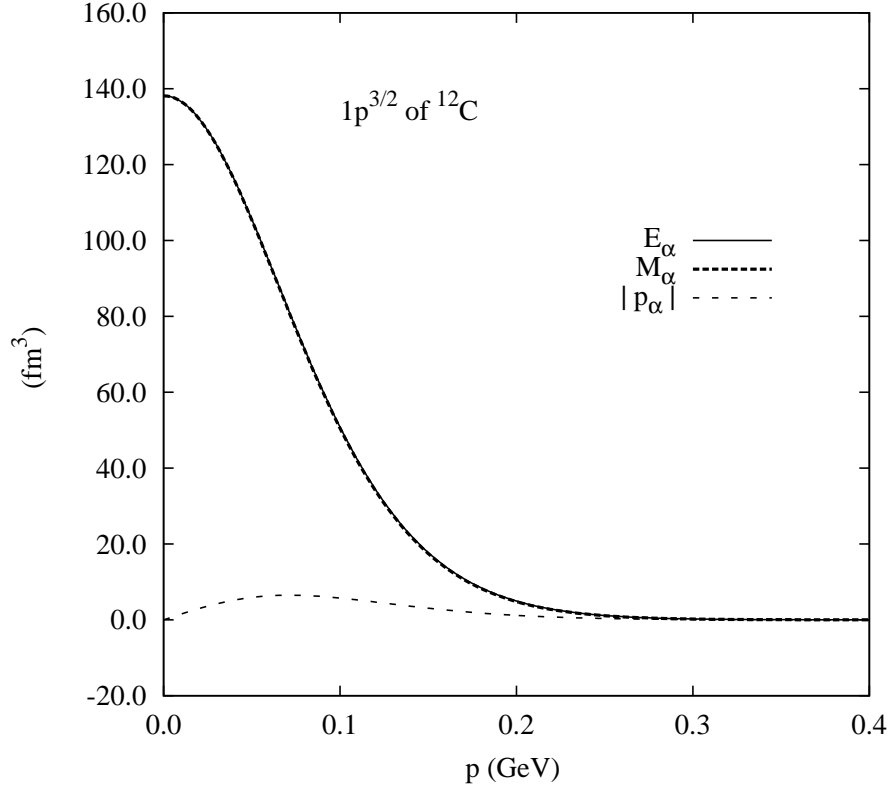


FIG. 3.8. The effective mass-, energy, and momentum-like quantities: M_{α} , E_{α} and \mathbf{p}_{α} as a function of the momentum (p)

free Dirac spinor given by

$$\mathcal{U}(\mathbf{p}'_2, s'_2) = \left(\frac{E_{p'_2} + M_{\Lambda}}{2E_{p'_2}} \right)^{\frac{1}{2}} \begin{pmatrix} 1 \\ \frac{\vec{\sigma} \cdot \mathbf{p}'_2}{E_{p'_2} + M_{\Lambda}} \end{pmatrix} \phi(s'_2). \quad (3.48)$$

Now we can write a tractable form of the hadronic tensor for the elementary process as

$$\begin{aligned} W^{\mu\nu} &= \sum_m \sum_{s'_2} \left[\bar{\mathcal{U}}(\mathbf{p}'_2, s'_2) \hat{J}^{\mu}(q) \mathcal{U}_{\alpha,m}(\mathbf{p}_m) \right] \left[\bar{\mathcal{U}}(\mathbf{p}'_2, s'_2) \hat{J}^{\nu}(q) \mathcal{U}_{\alpha,m}(\mathbf{p}_m) \right]^* \\ &= \sum_m \sum_{s'_2} \left\{ \bar{\mathcal{U}}(\mathbf{p}'_2, s'_2) \left(\sum_{i=1}^6 A_i \mathcal{M}_i^{\mu} \right) \mathcal{U}_{\alpha,m}(\mathbf{p}_m) \right\} \\ &\quad \times \left\{ \bar{\mathcal{U}}(\mathbf{p}'_2, s'_2) \left(\sum_{j=1}^6 A_j \mathcal{M}_j^{\nu} \right) \mathcal{U}_{\alpha,m}(\mathbf{p}_m) \right\}^{\dagger}. \end{aligned} \quad (3.49)$$

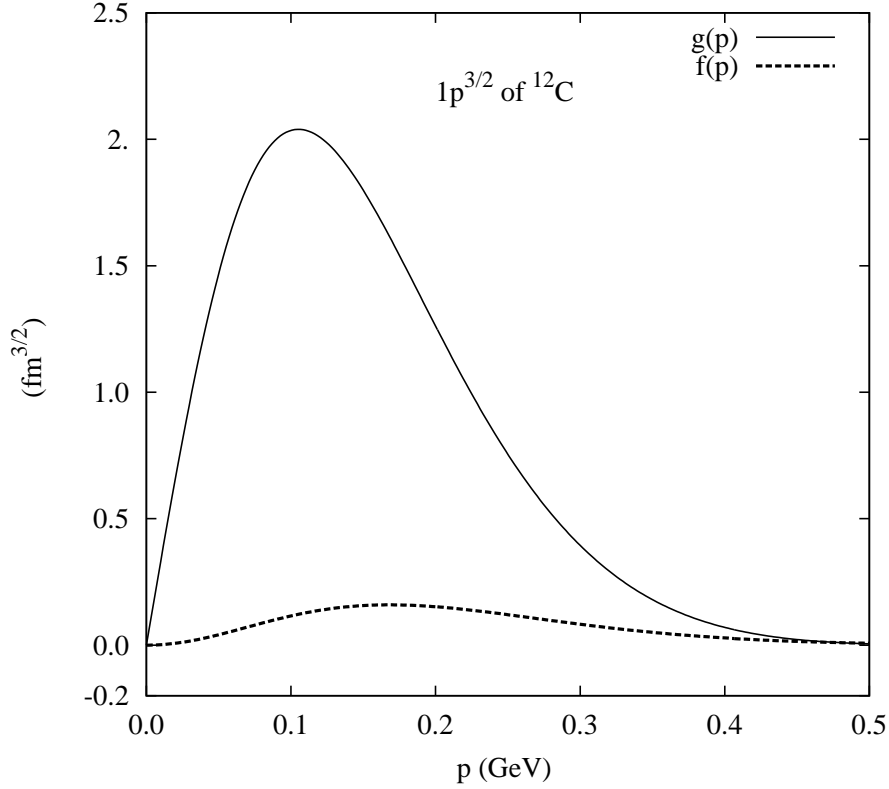


FIG. 3.9. The radial component $g_\alpha(p)$ and $g_\alpha(p)$ of the wave function of the bound-nucleon (proton in our case) in momentum space for orbital $1p_{3/2}$ of the ^{12}C nucleus

Using the properties of matrix multiplication and recalling the Casimir method Eq. (3.42), and the Gardner and Piekarewicz method Eq. (3.45), the hadronic tensor can be written as [see Appendix C]

$$W^{\mu\nu} = \frac{2j+1}{2E_{p'_2}} \sum_{i,j=1}^6 A_i A_j^* \text{Tr} \left[\mathcal{M}_i^\mu (\not{p}'_\alpha + M_\alpha) \overline{\mathcal{M}}_i^\nu (\not{p}'_2 + M_2) \right], \quad (3.50)$$

where $\overline{\mathcal{M}}_i^\mu = \gamma^0 (\mathcal{M}_i^\mu)^\dagger \gamma^0$. Now we are in position to employ powerful trace algebra techniques developed by Feynman to compute all observables, and using the invariant amplitudes provided by the model and the six Lorentz- and gauge-invariant quantities given in Eqs. (3.35a) - (3.35f). Then the hadronic tensor can be written as

$$W^{\mu\nu} = \frac{2j+1}{2E_{p'_2}} \sum_{i,j=1}^6 w_{ij}^{\mu\nu}, \quad (3.51)$$

where $w_{ij}^{\mu\nu}$ is a particular combination of i and j . For example,

$$\begin{aligned} w_{11}^{\mu\nu} &= |A_1|^2 \text{Tr} \left[\mathcal{M}_1^\mu (\not{p}_\alpha + M_\alpha) \overline{\mathcal{M}_1^\nu} (\not{p}'_2 + M'_2) \right] \\ &= \frac{|A_1|^2}{4} \text{Tr} \left[\gamma^5 (\gamma^\mu \not{q} - \not{q} \gamma^\mu) (\not{p}_\alpha + M_\alpha) (\gamma^\nu \not{q} - \not{q} \gamma^\nu) \gamma^5 (\not{p}'_2 + M'_2) \right], \end{aligned} \quad (3.52)$$

which gives

$$\begin{aligned} w_{11}^{\mu\nu} &= |A_1|^2 \times \left[q^2 (p_\alpha^\mu p_2'^\nu + p_2'^\mu p_\alpha^\nu - [p_2' \cdot p_\alpha - M_\alpha M'_2] g^{\mu\nu}) \right. \\ &\quad - (q \cdot p_\alpha) (q^\mu p_2'^\nu + p_2'^\mu q^\nu - (q \cdot p_2') g^{\mu\nu}) \\ &\quad - (q \cdot p_2') (q^\mu p_\alpha^\nu + p_\alpha^\mu q^\nu - (q \cdot p_\alpha) g^{\mu\nu}) \\ &\quad \left. + (p_2' \cdot p_\alpha - M_\alpha M'_2) q^\mu q^\nu \right]. \end{aligned} \quad (3.53)$$

Detailed expressions of all quantities $w_{ij}^{\mu\nu}$ are presented in appendix C.

Chapter 4

Results

The results that will be presented in this work is related with the application of the formalism developed in chapter three. The calculation of the hadronic tensor is relatively complex, but with the approximations already made we are able to calculate the hadronic tensor for the elementary electromagnetic production of pseudo-scalar-meson and hyperon process

$$e + A \longrightarrow e + K^+ + \Lambda + A_{\text{res}} . \quad (4.1)$$

Since the hadronic tensor depends strongly on the behaviour of the bound state wave function and the binding energy of the bound nucleon, it is interesting to consider different nuclei and different orbital levels.

4.1 Kinematic setup

The kinematic setup for the electromagnetic production of pseudoscalar mesons and free hyperons is very complicated to deal with, since the kinematics depend on various quantities. We first make use of energy conservation

$$E_k + M_A = E_{k'} + E_{p'_1} + E_{p'_2} + E_{P'} , \quad (4.2)$$

in order to simplify the δ -function in the relation for the differential cross section [see Eq. (3.5)]. In the laboratory frame the total energy of the recoil nucleus is given by

$$E_{P'} = \sqrt{\mathbf{P}'^2 + M_{A-1}^2} = \sqrt{(\mathbf{q} - \mathbf{p}'_1 - \mathbf{p}'_2)^2 + M_{A-1}^2} , \quad (4.3)$$

where M_A is the mass of the target nucleus, M_{A-1} the mass of the recoil nucleus, M_p is the mass of the bound nucleon. The proton mass and the binding energy of the bound nucleon E_b are related as follows:

$$M_{A-1} = M_A - (M_p - E_b). \quad (4.4)$$

The δ -function can be written as a function of only one kinematic variable. In our case, we have chosen the hyperon energy $E_{p'_2}$

$$\delta(E_k + M - E_{k'} - E_{p'_1} - E_{p'_2} - E_{P'}) \equiv \delta(f[E_{p'_2}]). \quad (4.5)$$

The complete evaluation of $f[E_{p'_2}]$ is provided in appendix A. The tractable kinematic setup was made possible by use of the solution of the quadratic equation

$$f[E_{p'_2}] = 0, \quad (4.6)$$

that gives and fixes the acceptable values for different input parameters such as the incident and scattered electron energies and angles, the produced kaon angle and energy, the unbound hyperon outgoing angle, etc ... In Table 4.1, we present the acceptable kinematics used for this work. Note that these values have been fixed using only one orbital namely the orbital $1p_{3/2}$ of the ^{12}C nucleus. By fixing the value of the incoming and outgoing

$E_k(\text{GeV})$	$E_{k'}(\text{GeV})$	$E_{p'_1}(\text{MeV})$	$\theta(\text{deg})$	$\theta'_1(\text{deg})$
3 – 5	2 – 4	500 – 1500	$0 \leq \theta \leq 15$	$0 \leq \theta'_1 \leq 20$

TABLE. 4.1. Acceptable kinematics

electron energies E_k and $E_{k'}$, the electron scattering angle θ_e , the produced kaon angle θ_{K^+} and energy $E_{p'_1}$, the angle between the leptonic and the hadronic planes ϕ , we are able to compute the value of the outgoing hyperon as a function of the hyperon outgoing angle θ_Λ . Once we get the value of the hyperon energy, this allows us to construct the hyperon four vector [see Eq. (3.16)].

Next we construct the bound nucleon four-vector using the approximation made in Sec. 3.5.2, where the bound nucleon has a four-momentum is given by

$$p = p'_1 + p'_2 - q. \quad (4.7)$$

The magnitude of the three-momentum of this quantity is used to compute the mass-, energy and momentum-like quantities given by Eqs. (3.46a - 3.46c). Hence, by constructing these quantities one is able to calculate the hadronic tensor which takes in account the bound state wave function of the bound nucleon.

In the formalism developed in this work, nuclear structure effects enter exclusively in terms of the momentum distribution of the bound nucleon. We make use of a relativistic mean-field approximation to compute the momentum distribution. In particular, we employed the FSUGold parameter set [47]. The hadronic tensor is calculated using the formalism described in Sec. 3.5.2. Since the momentum distribution depends on the missing momentum, which itself depends on the momentum of the virtual photon, the produced kaon and the outgoing free hyperon, it is difficult to find a suitable set of these values. We first fixed the incident electron energy at 3 GeV corresponding to the beam energy used at JLab and scattered electron energy of 2 GeV, the electron scattering angle was fixed to 5° and the kaon angle to 10° . Then we calculate the hyperon energy as function of the hyperon angle from 0° to 180° , for each single orbital for the nuclei used in this work, namely the ^{12}C , ^{16}O , ^{40}Ca and ^{208}Pb . Since the momentum space wave function of the bound nucleon (proton for our case) is only appreciable for the missing momentum $p \leq 300\text{MeV}$, the differential cross section is also affected by this condition. This will be seen later on in our results. In Fig. 4.1 we present the momentum distribution of the bound nucleon for the orbitals $1s_{1/2}$ and $1p_{3/2}$ of the ^{12}C nucleus, for a kaon energy of 700 MeV and 720 MeV. This is done for all nuclei of interest. The results for ^{16}O are presented in Fig. 4.2.

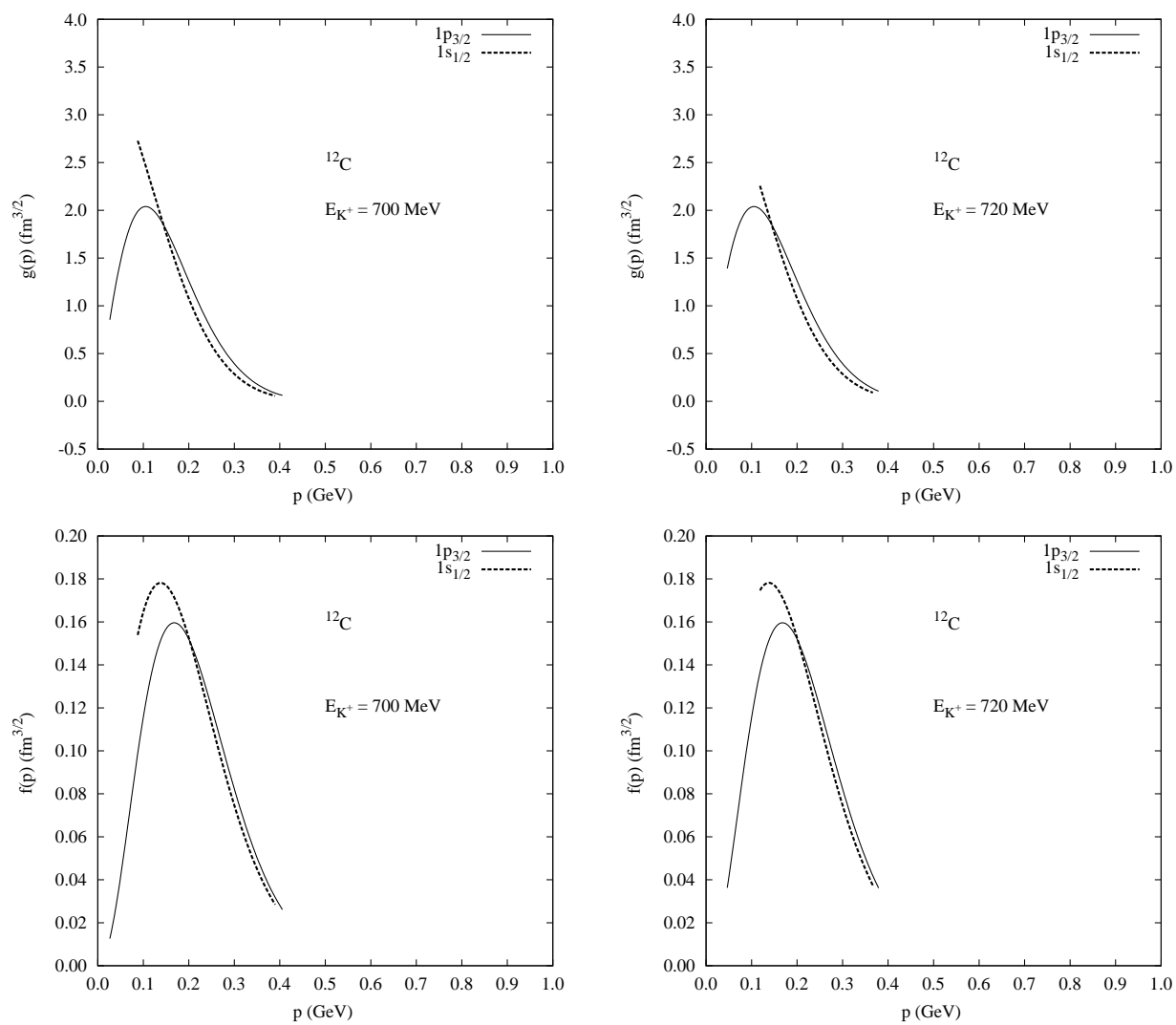


FIG. 4.1. Upper $g(p)$ and lower $f(p)$ components of the proton bound state wave-function in the momentum space for the orbitals $1s_{1/2}$ and $1p_{3/2}$ of ^{12}C for $E_{K^+}=700$ MeV and 720 MeV

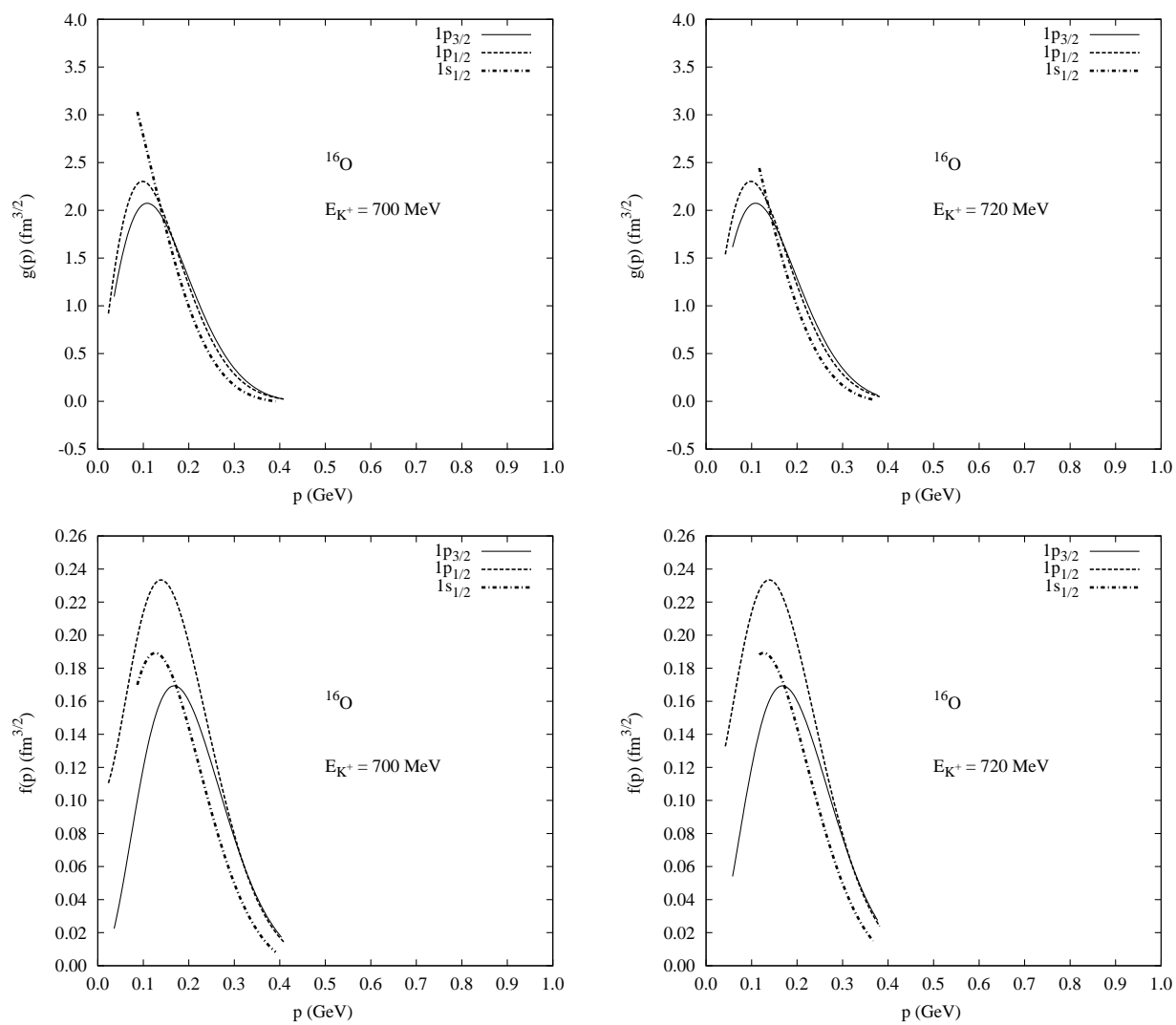


FIG. 4.2. Upper $g(p)$ and lower $f(p)$ components of the proton bound state wave-function in the momentum space for the orbitals $1s_{1/2}$, $1p_{3/2}$ and $1p_{1/2}$ of ^{16}O for $E_{K^+} = 700$ MeV and 720 MeV

We can see in these figures how the momentum distribution decreases with kaon energy. This gives an indication of the behaviour of the differential cross section, since the momentum distribution of the bound nucleon plays a dominant role. The orbital $1p_{3/2}$ has an important contribution to the differential cross section compared to the contribution of orbital $1s_{1/2}$. We present the results of the different combinations for the differential cross section. To compare the influence of the nucleon distributions within orbitals we present our results for different orbital levels in the nucleus, using the four nuclei considered in this work. According to the shell model the ^{12}C nucleus has six protons distributed as two protons bound in the orbital $1s_{1/2}$ with a binding energy of 39.19 MeV and four protons to the orbital $1p_{3/2}$ with 13.69 MeV binding energy, Table 4.2 gives the shell structure of the orbitals and binding energies for the ^{12}C nucleus.

Orbitals	j	l	Kappa (κ)	Proton number	E_b (MeV)
$1s_{1/2}$	1/2	0	-1	2	39.19
$1p_{3/2}$	3/2	1	-2	4	13.69

TABLE. 4.2. Shell structure parameters of ^{12}C for relativistic mean-field model

Fixing the electron scattering angle θ_e , the produced kaon energy $E_{p'_1}$ and angle θ_{K}^+ , we compute the outgoing hyperon energy $E_{p'_2}$ as the solution of the equation Eq. (4.6) for different hyperon angles. We first present in Figs. [(4.3) and (4.4)], the behaviour of the differential cross section for different energy transfers for the orbital $1s_{1/2}$ and $1p_{3/2}$ of ^{12}C as function of the hyperon angle. These results show clearly that the peak of the differential cross section increases as the energy transfer increases and it is higher for the orbital with a large number of nucleons.

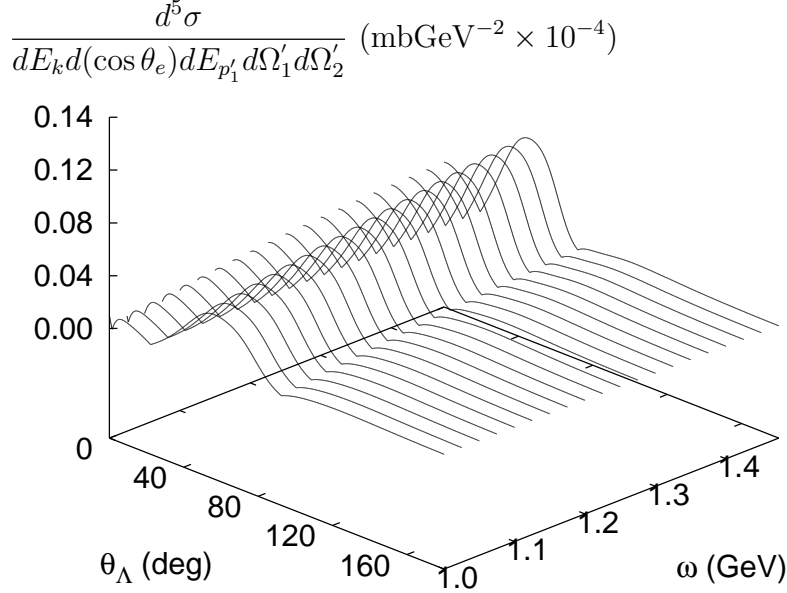


FIG. 4.3. The differential cross section for the electro-production of K^+ and unbound hyperon using the orbital $1s_{1/2}$ of the ^{12}C nucleus

More explicitly we present the results of the differential cross section for all considered nuclei showing the contribution of each orbital level. In Fig. 4.5 we present the result for ^{12}C and ^{16}O nuclei. ^{16}O has eight protons distributed as two in $1s_{1/2}$, four in $1p_{3/2}$ and two in $1p_{1/2}$ or orbitals with 38.92 MeV, 18.36 MeV, 11.99 MeV binding energies respectively: Table 4.3 gives the shell structure of the orbitals and binding energies for the ^{16}O nucleus.

In Fig. ??, we display the differential cross section contributions for the orbitals $1p_{1/2}$ and $1p_{3/2}$ of ^{16}O nucleus as function of outgoing hyperon angle. In these results we see that for example the $1p_{3/2}$ orbital of ^{12}C nucleus has a dominant contribution than the orbital $1p_{3/2}$. This also happened for the ^{16}O nucleus, in this case the dominant orbital is the $1p_{1/2}$ which has also the lower binding energy followed by the $1p_{3/2}$. That can be an indication that the reaction take place in prior in the lastest orbital according to the shell structure parameters for relativistic mean-field model. We also emphasize that the peak of the

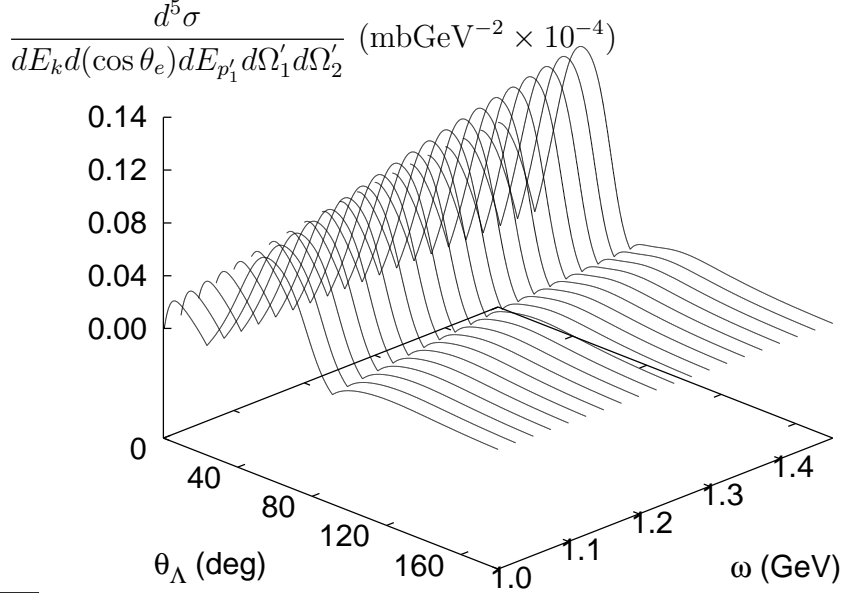


FIG. 4.4. The differential cross section for the electro-production of K^+ and unbound hyperons using the orbital $1p_{3/2}$ of the ^{12}C nucleus

Orbitals	j	l	Kappa (κ)	Proton number	E_b (MeV)
$1s_{1/2}$	1/2	0	-1	2	38.92
$1p_{3/2}$	3/2	1	-2	4	18.36
$1p_{1/2}$	1/2	1	+1	2	11.99

TABLE. 4.3. Shell structure parameters of the ^{16}O for relativistic mean-field model

differential cross section has a high value for a high energy transfer to the bound nucleon and also that this peak becomes narrower as we increase the energy transfer.

The ^{40}Ca nucleus has 20 protons distributed as two in $1s_{1/2}$, four in $1p_{3/2}$, two in $1p_{1/2}$, six in $1d_{5/2}$, two in $2s_{1/2}$ and four in the $1d_{3/2}$ orbitals. Table 4.4 gives the shell structure of the orbitals and binding energies for the ^{40}Ca nucleus.

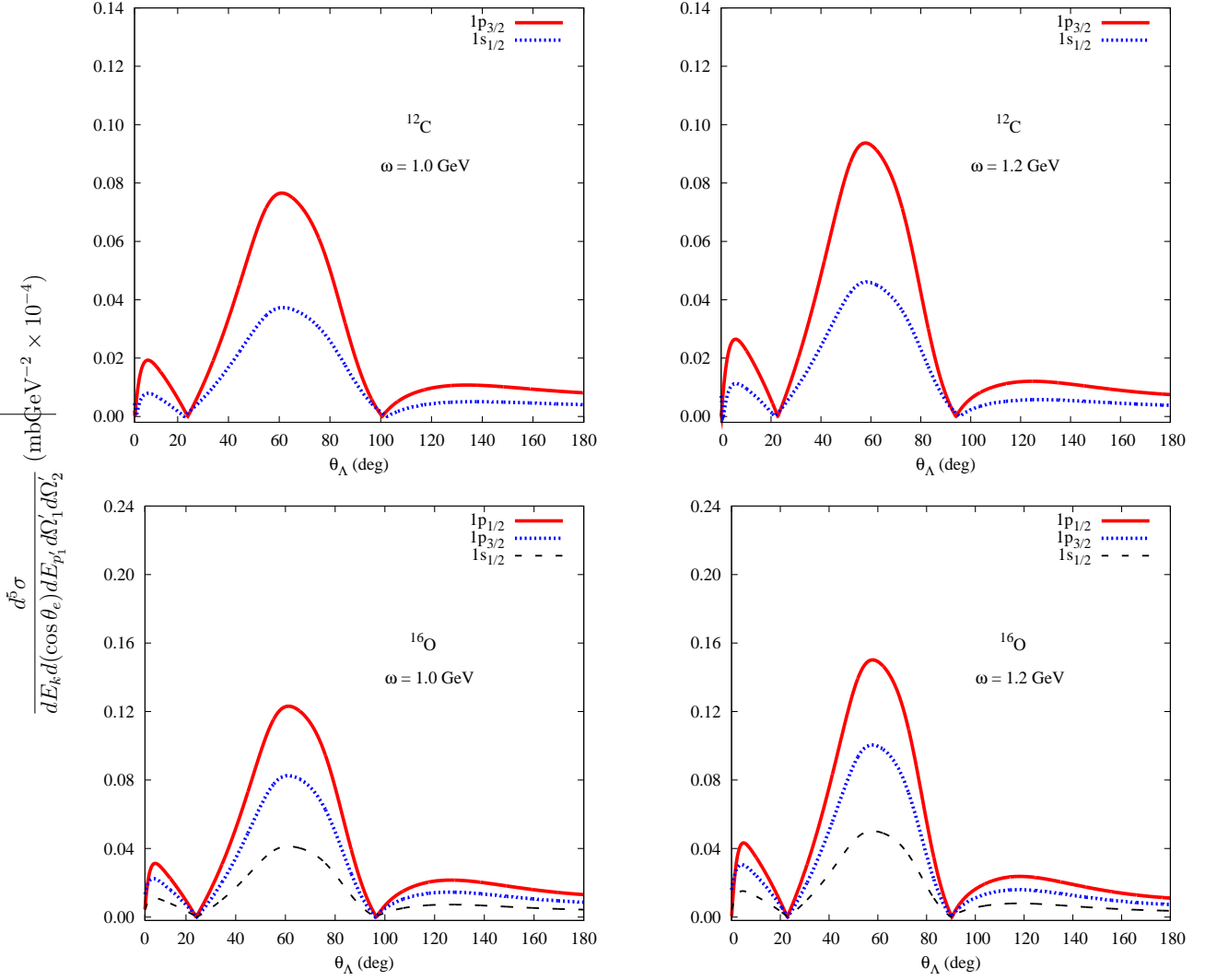


FIG. 4.5. Differential cross section for the K^+ electro-production with free hyperon from the ^{12}C nucleus (top), using the orbital $1s_{1/2}$ and $1p_{3/2}$, and ^{16}O (bottom), the orbital $1s_{1/2}$ and $1p_{3/2}$ using the orbital $1s_{1/2}$, $1p_{3/2}$ and $1p_{1/2}$ for different energies transfer ω

The results for ^{40}Ca present in Fig 4.6 confirm our previous discussion, the results follow the shell structure parameters for relativistic mean-field model. The contribution to the differential cross section follows this decreasing order of the shell structure, i.e. $1d_{3/2}$, $2s_{1/2}$, $1d_{5/2}$, $1p_{1/2}$, $1p_{3/2}$ and $1s_{1/2}$.

Orbitals	j	l	Kappa (κ)	Proton number	E_b (MeV)
$1s_{1/2}$	1/2	0	-1	2	46.17
$1p_{3/2}$	3/2	1	-2	4	30.84
$1p_{1/2}$	1/2	1	+1	2	27.05
$1d_{5/2}$	5/2	2	-3	6	15.58
$2s_{1/2}$	1/2	0	-1	2	9.31
$1d_{3/2}$	3/2	2	+2	4	9.30

TABLE. 4.4. Shell structure parameters of ^{40}Ca for relativistic mean-field model

The ^{208}Pb nucleus contains about sixteen orbital levels: Table 4.5 gives the shell structure of the orbitals and binding energies for ^{208}Pb . It is very difficult to display all orbital contributions in one figure, so we have grouped our results with respect to the shell structure for our relativistic mean-field model. The results of the differential cross section are presented in Figs. 4.7 and 4.8. We can see that the external orbital gives the dominant contribution to the differential cross section of the production process.

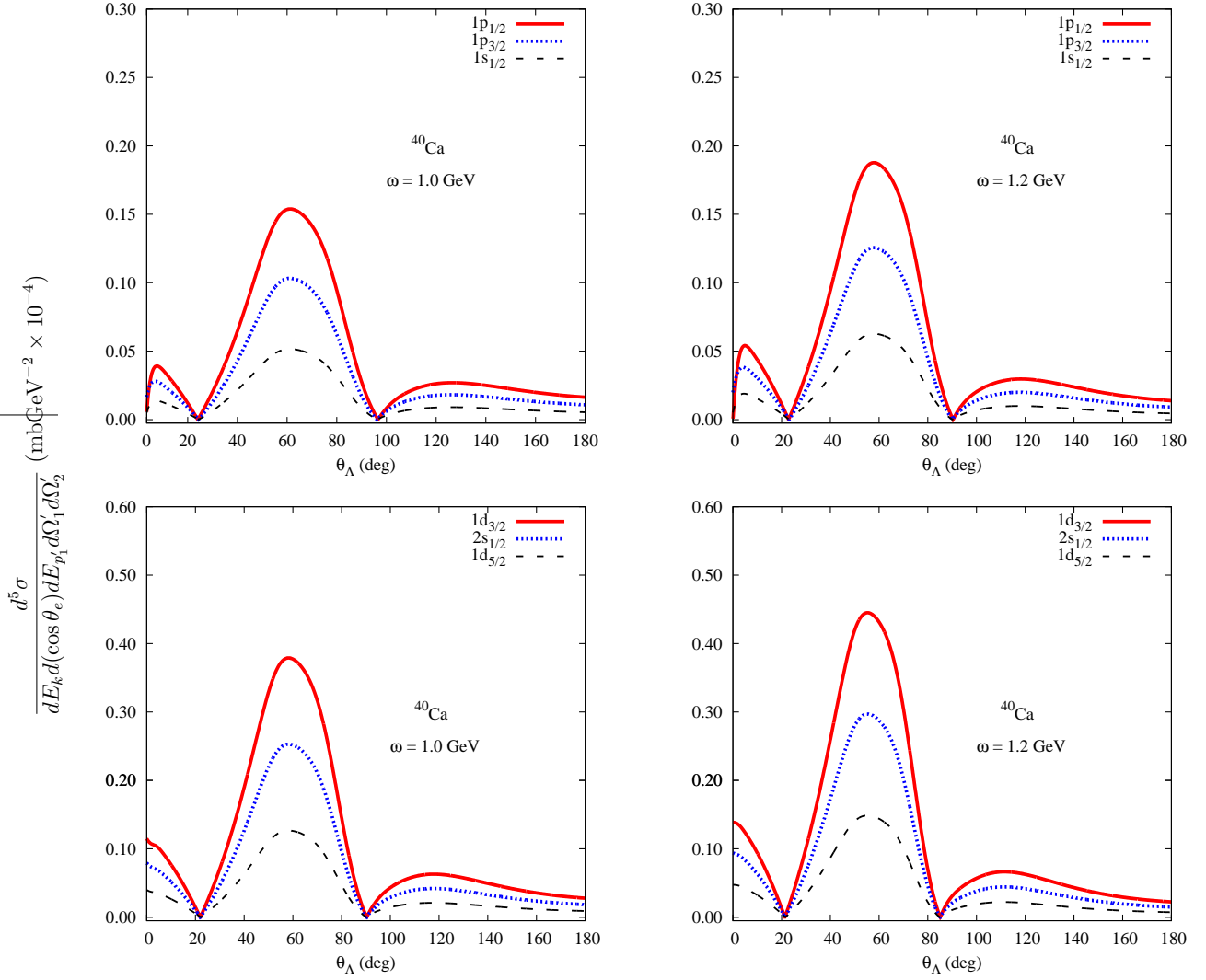


FIG. 4.6. Differential cross section for the K^+ electro-production with free hyperon from the ^{40}Ca nucleus, using the orbital $1s_{1/2}$, $1p_{3/2}$, $1p_{1/2}$ (top), and using the orbital $1d_{5/2}$, $1d_{3/2}$ and $2s_{1/2}$ (bottom), for different energies transfer ω

Orbitals	j	l	Kappa (κ)	Proton number	E_b (MeV)
$1s_{1/2}$	1/2	0	-1	2	48.00
$1p_{3/2}$	3/2	1	-2	4	42.58
$1p_{1/2}$	1/2	1	+1	2	41.99
$1d_{5/2}$	5/2	2	-3	6	35.74
$2s_{1/2}$	1/2	0	-1	2	30.57
$1d_{3/2}$	3/2	2	+2	4	34.38
$1f_{7/2}$	7/2	3	-4	8	27.86
$1f_{5/2}$	5/2	3	+3	6	25.43
$2p_{3/2}$	3/2	1	-2	4	20.61
$2p_{1/2}$	1/2	1	+1	2	19.60
$1g_{9/2}$	9/2	4	-5	10	19.28
$1g_{7/2}$	7/2	4	+4	8	15.52
$2d_{5/2}$	5/2	2	-3	6	10.80
$1h_{11/2}$	11/2	5	-6	12	10.26
$2d_{3/2}$	3/2	2	+2	4	9.18
$3s_{1/2}$	1/2	0	-1	2	8.02

TABLE. 4.5. Shell structure parameters of ^{208}Pb for relativistic mean-field model

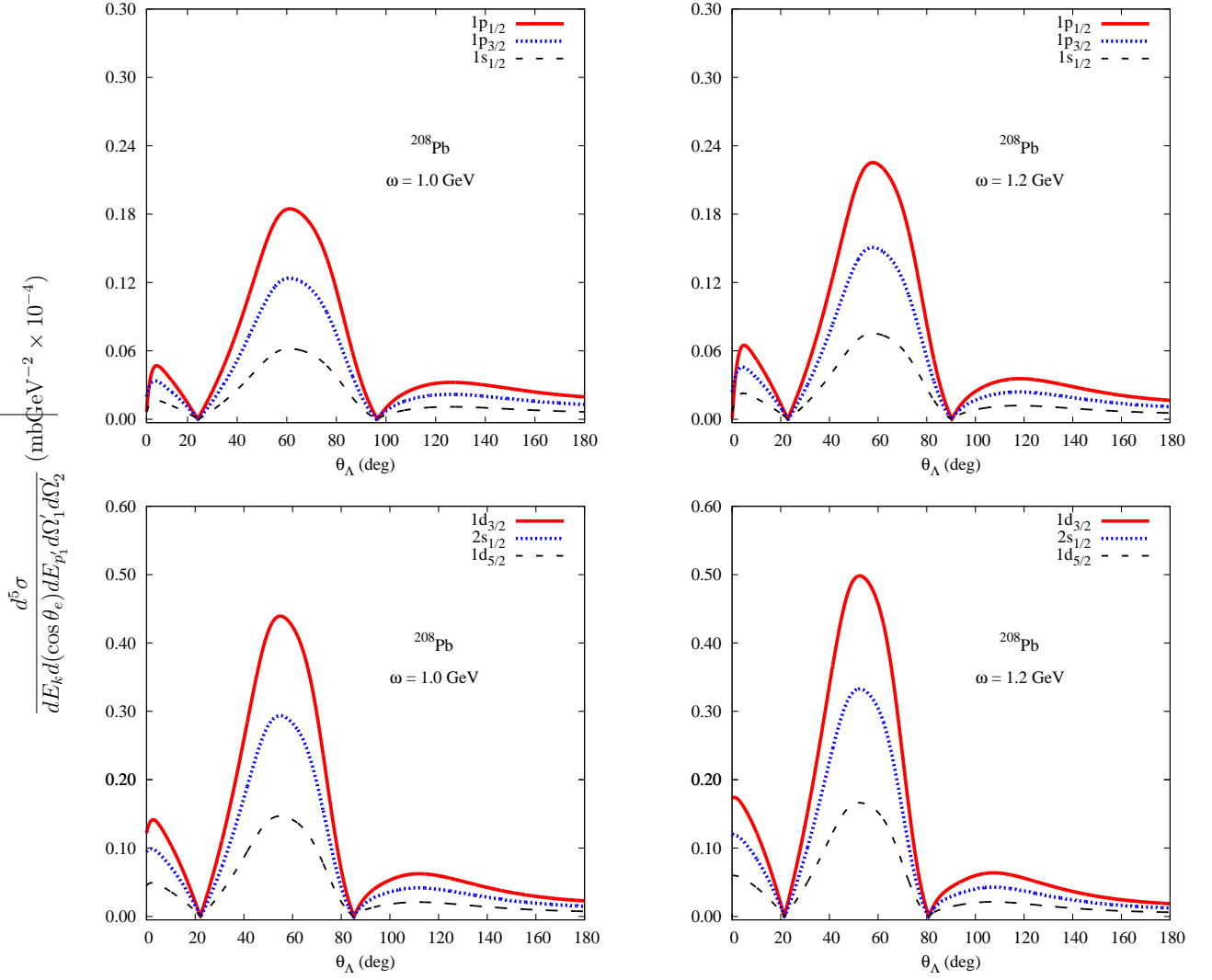


FIG. 4.7. Differential cross section for the K^+ electro-production with free hyperon from the ^{208}Pb nucleus, using the orbital $1s_{1/2}$, $1p_{3/2}$, $1p_{1/2}$, $1d_{5/2}$, $1d_{3/2}$ and $2s_{1/2}$ for different energies transfer ω

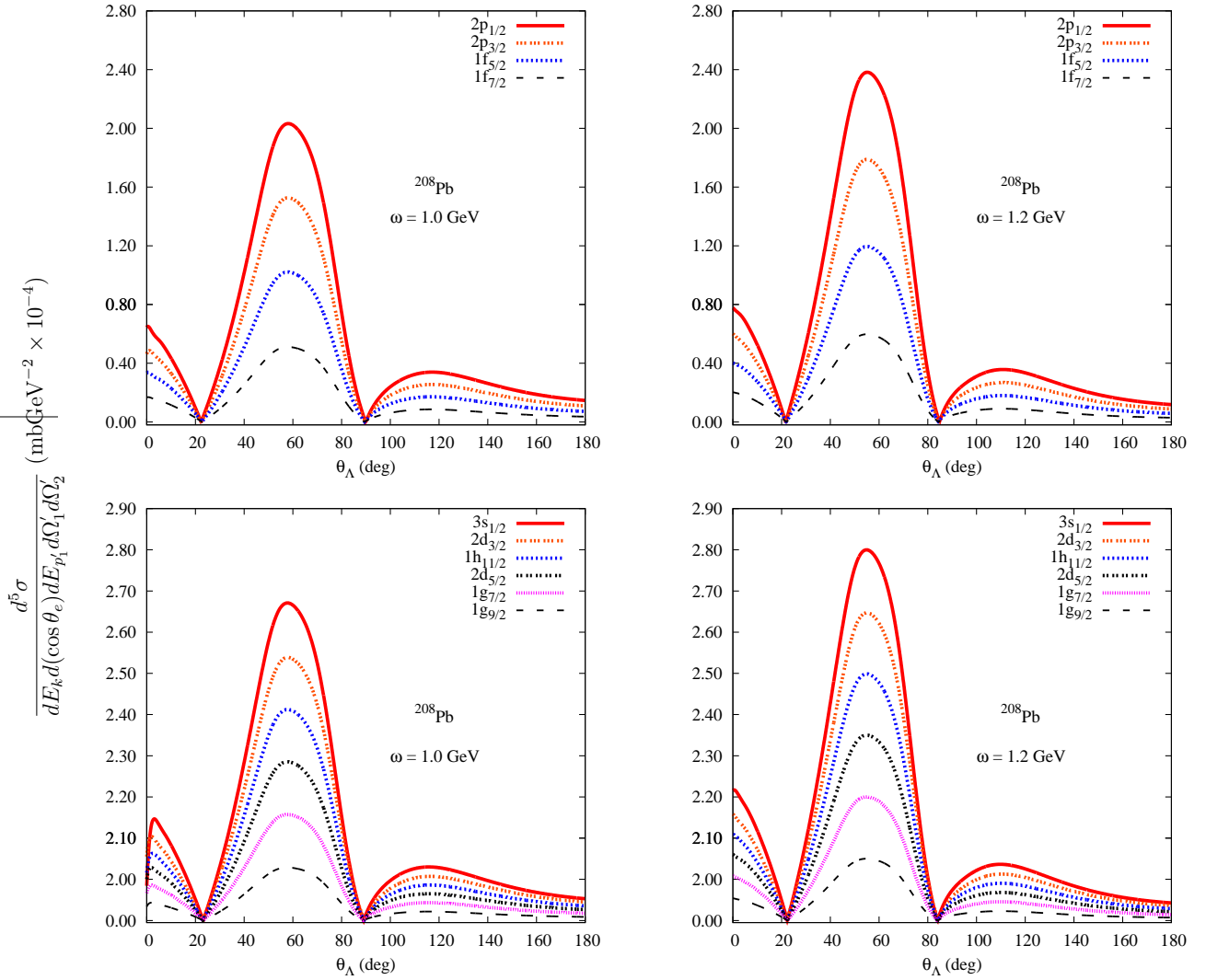


FIG. 4.8. Differential cross section for the K^+ electro-production with free hyperon from the ^{208}Pb nucleus, using the remaining orbitals from $1f_{7/2}$ to $3s_{1/2}$ in the shell structure for different energies transfer ω

Chapter 5

Summary and Conclusions

The results presented in this work represent one of the first attempts to investigate the behaviour of the differential cross section at the orbital level. We have developed a formalism for describing the electromagnetic production of pseudo-scalar mesons and unbound hyperons from nuclei, $A(e, e K^+ \Lambda)A_{\text{res}}$, and performed calculations in the quasifree regime. The formalism is based on the scattering process constituted by a leptonic part represented by the incident and scattered electron on one side, and the hadronic part represented by the target nucleus and the produced kaon and the Λ -hyperon on the other side. The relativistic mean-field model [39] has been used to extract the bound state wavefunction of the bound nucleon (proton).

The leptonic wavefunction is specified using a helicity representation of the free Dirac spinor in order to take in account the polarizability of the electron beam. The energy range was motivated by beam energies available at Jefferson lab. The dynamics of the process is written in terms of the transition matrix element which is expressed as a contraction of the leptonic tensor and the hadronic tensor. As shown in Appendix B, the leptonic tensor is evaluated using the helicity representation for a free Dirac spinor. The hadronic tensor is based on the model developed in Refs. [2, 50] as a linear combination of six invariant amplitudes and six Lorentz- and gauge-invariant quantities.

Our investigation mainly focused on the calculation of the unpolarized differential cross section for this production process, since this is the observable of primary interest to experimentalists. We use Fermi's golden rule to separate the kinematics to the dynamics

of the process. The kinematics setup is difficult to deal with, since the kinematics from the production process developed in this work depend on many parameters, namely the masses, energies and scattering angles of the interacting and produced particles. All information about the dynamics of the process is contained in the transition amplitude element which is written in terms of the leptonic tensor and the hadronic one. The nuclear structure calculations were performed using the relativistic mean field theory to the Walecka model. We made use of the FSUGold parameters set in this work for the bound state wave-function of bound nucleons.

We used Feynman diagrams and rules as well as trace algebra techniques to completely write down the expression of the transition matrix element for our production process. The valence orbital predicted by the shell structure for the relativistic mean-field model is well respected by our results. Our hope is that experimental data will be available in the near future to test our theoretical model.

Appendix A

Derivation of the Differential Cross section

The electro-production of pseudo-scalar-mesons from nuclei is represented by the following reaction:

$$A(e, e K^+ \Lambda) A_{\text{res}} \quad \text{or} \quad e + A \longrightarrow e + K^+ + \Lambda + A_{\text{res}} \quad (\text{A.1})$$

Let the position space representation of the free spin-0 particles be:

$$\phi(x) = N_V e^{-i\mathbf{p}\cdot\mathbf{x}} \quad (\text{A.2})$$

where N_V is a normalization constant that is concerned with the particle density and has nothing to do with the spinor normalization. The associated density is given by:

$$\rho = 2E |N_V|^2 . \quad (\text{A.3})$$

Let the position space representation of the spin- $\frac{1}{2}$ particles be given by:

$$\psi(x) = N_V u(\mathbf{p}, s) e^{-i\mathbf{p}\cdot\mathbf{x}} . \quad (\text{A.4})$$

The corresponding density is:

$$\rho = \psi^\dagger \psi ,$$

hence

$$\rho = |N_V|^2 u^\dagger(\mathbf{p}, s) u(\mathbf{p}, s) . \quad (\text{A.5})$$

We see that the spinor normalization is usual. Let now assume that:

$$u^\dagger(\mathbf{p}, s) u(\mathbf{p}, s) = C$$

where C is a constant, then

$$\rho = CN_V^2. \quad (\text{A.6})$$

The density satisfies

$$\begin{aligned} \rho &= \text{Number of particles per unit volume} \\ &= \frac{\text{Number of particles}}{V} \\ &= \frac{n}{V} \end{aligned}$$

Then

$$CN_V^2 = \frac{n}{V} \Rightarrow N_V = \sqrt{\frac{n}{CV}}. \quad (\text{A.7})$$

We now define the transition rate W_{fi} per unit volume or transition probability per unit time per unit volume:

$$W_{fi} = \frac{|T_{fi}|}{TV} \quad (\text{A.8})$$

where

$$T_{fi} = -i \overbrace{N_{V_1} N_{V_2} N_{V_3} N_{V_4} N_{V_5} N_{V_6}}^{\text{Normalization factor for each particle}} (2\pi)^4 \delta^4(k + P - k' - p'_1 - p'_2 - P') \mathcal{M}, \quad (\text{A.9})$$

then

$$\begin{aligned} W_{fi} &= \frac{(N_{V_1}^2 N_{V_2}^2 N_{V_3}^2 N_{V_4}^2 N_{V_5}^2 N_{V_6}^2)}{TV} [(2\pi)^4 \delta(k + P - k' - p'_1 - p'_2 - P')]^2 |\mathcal{M}|^2 \\ &= (N_{V_1}^2 N_{V_2}^2 N_{V_3}^2 N_{V_4}^2 N_{V_5}^2 N_{V_6}^2) (2\pi)^4 \delta^4(k + P - k' - p'_1 - p'_2 - P') |\mathcal{M}|^2. \end{aligned} \quad (\text{A.10})$$

Now we define:

$$d\sigma = \frac{W_{fi}}{\text{Initial flux}} (\text{Number of final states}) \frac{1}{V} \quad (\text{A.11})$$

The initial flux: $\frac{|\mathbf{v}_1 - \mathbf{v}_2|}{V}$ where $|\vec{v}_1 - \vec{v}_2|$ represents the relative velocity of the initial particles.

$$d\sigma = \frac{W_{fi} V^2}{|\vec{v}_1 - \vec{v}_2|} \left(\frac{V d^3 \mathbf{k}'}{n (2\pi)^3} \right) \left(\frac{V d^3 \mathbf{p}'_1}{n (2\pi)^3} \right) \left(\frac{V d^3 \mathbf{p}'_2}{n (2\pi)^3} \right) \left(\frac{V d^3 \mathbf{P}'}{n (2\pi)^3} \right) \quad (\text{A.12})$$

One can use

$$|\mathbf{v}_1 - \mathbf{v}_2| = \frac{4 [(k \cdot P)^2 - m_e^2 M^2]^{1/2}}{(2E_k)(2E_P)}, \quad (\text{A.13})$$

then

$$d\sigma = W_{fi} \left[\frac{V^2(2E_k)(2E_P)}{4 [(k \cdot P)^2 - m_e^2 M^2]^{1/2}} \right] \left(\frac{V d^3 \mathbf{k}'}{n (2\pi)^3} \right) \left(\frac{V d^3 \mathbf{p}'_1}{n (2\pi)^3} \right) \left(\frac{V d^3 \mathbf{p}'_2}{n (2\pi)^3} \right) \left(\frac{V d^3 \mathbf{P}'}{n (2\pi)^3} \right) (\text{A.14})$$

Using Eq. (A.10), the differential cross-section becomes:

$$d\sigma = \left[\frac{V^2(2E_k)(2E_P)}{4 [(k \cdot P)^2 - m_e^2 M^2]^{1/2}} \right] (2\pi)^4 \delta^4(k + P - k' - p'_1 - p'_2 - P') \quad (\text{A.15})$$

$$\times (N_{V_1}^2 N_{V_2}^2 N_{V_3}^2 N_{V_4}^2 N_{V_5}^2 N_{V_6}^2) \left(\frac{V d^3 \mathbf{k}'}{n (2\pi)^3} \right) \left(\frac{V d^3 \mathbf{p}'_1}{n (2\pi)^3} \right) \left(\frac{V d^3 \mathbf{p}'_2}{n (2\pi)^3} \right) \left(\frac{V d^3 \mathbf{P}'}{n (2\pi)^3} \right) |\mathcal{M}|^2.$$

Eq. (A.15) is very general. We now have to decide on:

1. How to normalize the boson density \implies Eq. (A.3)
2. How to normalize the fermion density \implies Eq. (A.5), which connected with spinor normalization.

Let's assume that the spinors are normalized to:

$$\bar{u}(\mathbf{p}, s) u(\mathbf{p}, s) = 1$$

then

$$u^\dagger(\mathbf{p}, s) u(\mathbf{p}, s) = \frac{E}{M} = C.$$

Let's assume we normalize the fermion to one particle per unit volume: $n = 1$, so

- $N_{V_1}^2 = \frac{m_e}{E_k V} \implies$ initial electron
- $N_{V_2}^2 = \frac{M}{E_P V} \implies$ initial nucleus
- $N_{V_3}^2 = \frac{m_e}{E'_k V} \implies$ outgoing electron
- $N_{V_5}^2 = \frac{M_\Lambda}{E_{p'_2} V} \implies$ unbound hyperon

- $N_{V_6}^2 = \frac{M'}{E_{P'}V} \implies$ recoil nucleus .

If we also normalize the bosons to one particle per unit volume then: $n = 1$, so

- $N_{V_4}^2 = \frac{1}{2E_{p'_1}V} \implies$ ejected pseudoscalar-meson .

Therefore the differential cross-section takes the form:

$$d\sigma = \left[\frac{V^2(2E_k)(2E_P)}{4[(k \cdot P)^2 - m_e^2 M^2]^{1/2}} \right] \left(\frac{m_e}{E_k V} \right) \left(\frac{M}{E_P V} \right) \left(\frac{m_e}{E'_k V} \right) \left(\frac{1}{2E_{p'_1} V} \right) \\ \times \left(\frac{M_p}{E_{p'_2} V} \right) \left(\frac{M'}{E_{P'} V} \right) \left(\frac{V d^3 \mathbf{k}'}{(2\pi)^3} \right) \left(\frac{V d^3 \mathbf{p}'_1}{(2\pi)^3} \right) \left(\frac{V d^3 \mathbf{p}'_2}{(2\pi)^3} \right) \left(\frac{V d^3 \mathbf{P}'}{(2\pi)^3} \right) \quad (\text{A.16})$$

$$(2\pi)^4 \delta^4(k + P - k' - p'_1 - p'_2 - P') |\mathcal{M}|^2$$

$$d\sigma = \frac{1}{(2\pi)^8} \frac{m_e^2 M M' M_p}{[(k \cdot P)^2 - m_e^2 M^2]^{1/2}} \frac{d^3 \mathbf{k}'}{E_{k'}} \frac{d^3 \mathbf{p}'_1}{2E_{p'_1}} \frac{d^3 \mathbf{p}'_2}{E_{p'_2}} \frac{d^3 \mathbf{P}'}{E_{P'}} \\ \times \delta^4(k + P - k' - p'_1 - p'_2 - P') |\mathcal{M}|^2 . \quad (\text{A.17})$$

For massless fermions the normalization is given by:

$$u^\dagger(\mathbf{p}, s) u(\mathbf{p}, s) = 1 = C ,$$

and the differential cross-section given by Eq. (A.17) becomes

$$d\sigma = \frac{1}{(2\pi)^8} d^3 \mathbf{k}' \frac{d^3 \mathbf{p}'_1}{2E_{p'_1}} d^3 \mathbf{p}'_2 d^3 \mathbf{P}' \delta^4(k + P - k' - p'_1 - p'_2 - P') |\mathcal{M}|^2 . \quad (\text{A.18})$$

We now can use the momentum conservation to establish an expression for the differential cross-section. Momentum conservation tells us that

$$\mathbf{k} + \mathbf{P} = \mathbf{k}' + \mathbf{p}'_1 + \mathbf{p}'_2 + \mathbf{P}'$$

then, since the recoil nucleus will not be observed, we can perform the integral over his momentum P' , using the fact that

$$\delta^4(k + P - k' - p'_1 - p'_2 - P') = \delta(E_k + M - E_{k'} - E_{p'_1} - E_{p'_2} - E_{P'}) \\ \times \delta^3(\mathbf{k} + \mathbf{P} - \mathbf{k}' - \mathbf{p}'_1 - \mathbf{p}'_2 - \mathbf{P}') . \quad (\text{A.19})$$

Therefore the differential cross-section Eq. (A.17) becomes

$$d\sigma = \frac{1}{(2\pi)^8} d^3\mathbf{k}' \frac{d^3\mathbf{p}'_1}{2E_{p'_1}} d^3\mathbf{p}'_2 \delta(E_k + M - E_{k'} - E_{p'_1} - E_{p'_2} - E_{P'}) |\mathcal{M}|^2. \quad (\text{A.20})$$

Now using the geometry of the process, we can write :

- $d^3\mathbf{k}' = (E_{k'} - m_e)^{1/2} E_{k'} dE_{k'} d\Omega_{k'} = 2\pi E_{k'}^2 dE_{k'} d(\cos\theta_e)$
- $d^3\mathbf{p}'_1 = (E_{p'_1} - M_{K^+})^{1/2} E_{p'_1} dE_{p'_1} d\Omega_{p'_1}$
- $d^3\mathbf{p}'_2 = (E_{p'_2} - M_\Lambda)^{1/2} E_{p'_2} dE_{p'_2} d\Omega_{p'_2}.$

Let's assume that our input is:

- M_P the nucleon (proton) mass
- M_Λ the mass of unbound hyperon
- M_{K^+} the free kaon mass
- θ_e the scattering angle of the electron
- θ_1 the ejected angle of mesons
- θ_2 the outgoing angle of hyperon
- $E_{k'}$ the energy of outgoing electron
- $E_{p'_1}$ the free meson energy
- ϕ angle between the leptonic and the hadronic planes

If we only detect the unbound hyperon, Eq. (A.20) can be written as

$$d\sigma = K \delta(E_k + M - E_{k'} - E_{p'_1} - E_{p'_2} - E_{P'}) dE_{k'} d(\cos\theta_e) dE_{p'_1} d\Omega_{p'_1} dE_{p'_2} d\Omega_{p'_2} |\mathcal{M}|^2 \quad (\text{A.21})$$

where K is a kinematic factor given by:

$$K = \frac{E_{k'}^2 E_{p'_2} (E_{p'_1}^2 - M_{K^+}^2)^{1/2} (E_{p'_2}^2 - M_\Lambda^2)^{1/2}}{2(2\pi)^7}.$$

Then

$$\frac{d^6\sigma}{dE_{k'}d(\cos\theta_e)dE_{p'_1}d\Omega_{p'_1}d\Omega_{p'_2}} = K\delta(E_k + M - E_{k'} - E_{p'_1} - E_{p'_2} - E_{P'})dE_{p'_2} |\mathcal{M}|^2, \quad (\text{A.22})$$

Let's now express the δ -function in Eq. (A.22) as a function of $E_{p'_2}$, the unbound hyperon energy. For this purpose we use energy conservation, namely

$$E_k + M = E_{k'} + E_{p'_1} + E_{p'_2} + E_{P'}.$$

Let us consider:

$$A = E_k + M - E_{k'} - E_{p'_1},$$

so that

$$\delta(E_k + M - E_{k'} - E_{p'_1} - E_{p'_2} - E_{P'}) \longrightarrow \delta(A - E_{p'_2} - E_{P'}). \quad (\text{A.23})$$

We know that $E_{P'} = \sqrt{\mathbf{P}'^2 + M'^2}$ and in the rest frame of the initial nucleus we have that:

$$\mathbf{P}' = \mathbf{k} - \mathbf{k}' - \mathbf{p}'_1 - \mathbf{p}'_2,$$

but

$$\mathbf{q} = \mathbf{k} - \mathbf{k}',$$

so

$$E_{P'} = \sqrt{(\mathbf{q} - \mathbf{p}'_1 - \mathbf{p}'_2)^2 + M'^2}. \quad (\text{A.24})$$

Performing $(\mathbf{q} - \mathbf{p}'_1 - \mathbf{p}'_2)^2$, we have to use the geometry of the process, and one can find:

$$(\mathbf{q} - \mathbf{p}'_1 - \mathbf{p}'_2)^2 = B_0 - 2B_2 |\mathbf{p}'_1| + |\mathbf{p}'_1|^2$$

where

$$B_0 = |\mathbf{q}|^2 + |\mathbf{p}'_1|^2 - 2\mathbf{q} \cdot \mathbf{p}'_1, \quad B_2 = |\mathbf{q}| \cos\theta_\Lambda - |\mathbf{p}'_1| \cos(\theta_\Lambda + \theta_{K^+}) \quad \text{and} \quad |\mathbf{p}'_2|^2 = E_{p'_2}^2 - M_\Lambda^2.$$

Then we can write

$$E_{P'} = [B_0 - 2B_2 \sqrt{E_{p'_2}^2 - M_\Lambda^2} + E_{p'_2}^2 - M_\Lambda^2 + M'^2]^{1/2}$$

or

$$E_{P'} = [B_1 - 2B_2 \sqrt{E_{p'_2}^2 - M_\Lambda^2} + E_{p'_2}^2]^{1/2}, \quad (\text{A.25})$$

with $B_1 = B_0 - M_\Lambda^2 + M'^2$. One can easily see that $E_{P'}$ is function of $E_{p'_2}$:

$$E_{P'} = g(E_{p'_2}). \quad (\text{A.26})$$

Substituting Eq. (A.26) in Eq. (A.23) we get

$$\delta(A - E_{p'_2} - E_{P'}) = \delta(A - E_{p'_2} - g(E_{p'_2})) = \delta(f(E_{p'_2})). \quad (\text{A.27})$$

Now the differential cross section Eq. (A.22) becomes

$$\frac{d^5\sigma}{dE_{k'}d\Omega_{k'}dE_{p'_1}d\Omega_{p'_1}d\Omega_{p'_2}} = K \delta[f(E_{p'_2})] dE_{p'_2} |\mathcal{M}|^2, \quad (\text{A.28})$$

which can be derived by using the following property of delta function:

$$\int dx \delta(f(x)) = \sum_k 1 / \left| \frac{df}{dx} \right|_{x_k}$$

with x_k the roots of $f(x)$ within the interval of integration. Let us consider $E_{p'_2} = z$, so

$$f(z) = A - z - g(z) = A - z - [B_1 - 2B_2(z^2 - M_\Lambda^2)^{1/2} + z^2]^{1/2}. \quad (\text{A.29})$$

Finding the roots of Eq. (A.29) $f(z) = 0$, we get the quadratic equation of form

$$A_0 z^2 + A_1 z + A_2 = 0$$

with

$$A_0 = 4(A^2 - B_2^2), \quad A_1 = -4A(A^2 - B_1), \quad A_2 = (A^2 - B_1)^2 - 4B_2^2 M_\Lambda^2.$$

Of these two solutions, only one will correspond to a physically acceptable value of the energy.

Appendix B

Leptonic tensor

In the following we want to derive the leptonic tensor using the helicity representation of free Dirac spinors $\bar{u}(\mathbf{k}, h)$ of momentum \mathbf{k} and helicity h . We know that the leptonic tensor can be written as,

$$L_{\mu\nu} = [\bar{u}(\mathbf{k}', h')\gamma_\mu u(\mathbf{k}, h)][\bar{u}(\mathbf{k}', h')\gamma_\nu u(\mathbf{k}, h)]^*, \quad (\text{B.1})$$

but

$$[\bar{u}(\mathbf{k}', h')\gamma_\nu u(\mathbf{k}, h)]^* = [\bar{u}(\mathbf{k}, h)\gamma_\nu u(\mathbf{k}', h')], \quad (\text{B.2})$$

so Eq. (B.1) becomes,

$$L_{\mu\nu} = [\bar{u}(\mathbf{k}', h')\gamma_\mu u(\mathbf{k}, h)][\bar{u}(\mathbf{k}, h)\gamma_\nu u(\mathbf{k}', h')], \quad (\text{B.3})$$

or this can be expressed in terms of a trace as:

$$L_{\mu\nu} = \text{Tr}[\gamma_\mu (u(\mathbf{k}, h)\bar{u}(\mathbf{k}, h)) \gamma_\nu (u(\mathbf{k}', h')\bar{u}(\mathbf{k}', h'))]. \quad (\text{B.4})$$

The helicity representation of a free Dirac spinor is given by

$$\mathcal{U}(\mathbf{k}, h) = \left(\frac{E_k + M}{2E_k}\right)^{1/2} \begin{pmatrix} \phi_h(\hat{\mathbf{k}}) \\ \frac{h|\mathbf{k}|}{E_k + M}\phi_h(\hat{\mathbf{k}}) \end{pmatrix}, \quad (\text{B.5})$$

or for the massless leptons

$$\mathcal{U}(\mathbf{k}, h) = \frac{1}{\sqrt{2}} \begin{pmatrix} \phi_h(\hat{\mathbf{k}}) \\ h\phi_h(\hat{\mathbf{k}}) \end{pmatrix}, \quad (\text{B.6})$$

where the matrix $\phi_h(\hat{\mathbf{k}})$ is given by

$$\phi_h(\hat{\mathbf{k}}) = \begin{pmatrix} (\cos \frac{\theta}{2})\delta_{h,1} - e^{-i\phi}(\sin \frac{\theta}{2})\delta_{h,-1} \\ e^{i\phi}(\sin \frac{\theta}{2})\delta_{h,1} + (\cos \frac{\theta}{2})\delta_{h,-1} \end{pmatrix}. \quad (\text{B.7})$$

Using the Eq. (B.6) and Eq. (B.7), we obtain the following identity

$$\mathcal{U}(\mathbf{k}, h)\bar{\mathcal{U}}(\mathbf{k}, h) = \frac{1}{4E} \not{k}[(I_4 - h\gamma^5)]. \quad (\text{B.8})$$

Let us first use Eq. (B.8) to derive an expression of the leptonic tensor for the massless case.

Let define the following,

i) $L_{\mu\nu}^{(0)}$ as the completely unpolarized leptonic tensor given by,

$$L_{\mu\nu}^{(0)} = \text{Tr}[\gamma_\mu \sum_{h=\pm 1} (u(\mathbf{k}, h)\bar{u}(\mathbf{k}, h)) \gamma_\nu \sum_{h'=\pm 1} (u(\mathbf{k}', h')\bar{u}(\mathbf{k}', h'))],$$

which means that both incoming and outgoing leptons are unpolarized. So we have,

$$\begin{aligned} L_{\mu\nu}^{(0)} &= \text{Tr}[\gamma_\mu \sum_{h=\pm 1} (u(\mathbf{k}, h)\bar{u}(\mathbf{k}, h)) \gamma_\nu \sum_{h'=\pm 1} (u(\mathbf{k}', h')\bar{u}(\mathbf{k}', h'))] \\ &= \text{Tr}[(\frac{1}{2E_k}\gamma_\mu \not{k})(\frac{1}{2E_{k'}}\gamma_\nu \not{k}')] \\ &= \frac{1}{4E_k E_{k'}} \text{Tr}[\gamma_\mu \not{k}\gamma_\nu \not{k}'] \\ &= \frac{1}{E_k E_{k'}} [k_\mu k'_\nu + k'_\mu k_\nu - g_{\mu\nu} k \cdot k'] \end{aligned} \quad (\text{B.9})$$

ii) $L_{\mu\nu}^{(1)}$ as a first partial polarization, when only the incoming beam is polarized, we have

$$\begin{aligned} L_{\mu\nu}^{(1)} &= \text{Tr}[\gamma_\mu (u(\mathbf{k}, h)\bar{u}(\mathbf{k}, h)) \gamma_\nu \sum_{h'=\pm 1} (u(\mathbf{k}', h')\bar{u}(\mathbf{k}', h'))] \\ &= \text{Tr} \left[\frac{1}{2E_k} \gamma_\mu \not{k} (\frac{1}{2}(I_4 - h\gamma^5)) \gamma_\nu \frac{1}{2E_{k'}} \not{k}' \right] \\ &= \frac{1}{8E_k E_{k'}} \text{Tr} [\gamma_\mu \not{k}\gamma_\nu \not{k}' - h\gamma_\mu \not{k}\gamma^5\gamma_\nu \not{k}'] \\ &= \frac{1}{8E_k E_{k'}} [\text{Tr}(\gamma_\mu \not{k}\gamma_\nu \not{k}') - h\text{Tr}(\gamma^5\gamma_\mu \not{k}\gamma_\nu \not{k}')] \\ &= \frac{1}{2E_k E_{k'}} [k_\mu k'_\nu + k'_\mu k_\nu - g_{\mu\nu} k \cdot k' - ihk^\alpha k'^\beta \epsilon_{\mu\nu\alpha\beta}] \\ &= \frac{1}{2} L_{\mu\nu}^{(0)} - \frac{ih}{2E_k E_{k'}} k^\alpha k'^\beta \epsilon_{\mu\nu\alpha\beta}. \end{aligned} \quad (\text{B.10})$$

Note that $L_{\mu\nu}^{(1)} = L_{\mu\nu}^{(1)}(k, k', h)$.

iii) $L_{\mu\nu}^{(2)}$ as the second partial polarization, when only the outgoing beam is polarized, we have,

$$L_{\mu\nu}^{(2)} = \text{Tr}[\gamma_\mu \sum_{h=\pm 1} (u(\mathbf{k}, h)\bar{u}(\mathbf{k}, h)) \gamma_\nu (u(\mathbf{k}', h')\bar{u}(\mathbf{k}', h'))], \quad (\text{B.11})$$

and we can show that $L_{\mu\nu}^{(2)} = L_{\mu\nu}^{(1)}(k, k', h')$. So we obtain,

$$L_{\mu\nu}^{(2)} = \frac{1}{2} L_{\mu\nu}^{(0)} - \frac{ih'}{2E_k E_{k'}} k^\alpha k'^\beta \epsilon_{\mu\nu\alpha\beta}, \quad (\text{B.12})$$

iv) $L_{\mu\nu}$ the complete tensor, when the both incoming and outgoing leptons are polarized:

$$\begin{aligned} L_{\mu\nu} &= \text{Tr}[\gamma_\mu (u(\mathbf{k}, h)\bar{u}(\mathbf{k}, h)) \gamma_\nu (u(\mathbf{k}', h')\bar{u}(\mathbf{k}', h'))] \\ &= \frac{1}{16E_k E_{k'}} \text{Tr} [\gamma_\mu \not{k} \gamma_\nu \not{k}' - h\gamma^5 \gamma_\mu \not{k} \gamma_\nu \not{k}' - h'\gamma^5 \gamma_\mu \not{k} \gamma_\nu \not{k}' + hh' \gamma_\mu \not{k} \gamma_\nu \not{k}'] \\ &= \frac{1}{16E_k E_{k'}} [(1 + hh') \text{Tr}(\gamma_\mu \not{k} \gamma_\nu \not{k}') - (h + h') \text{Tr}(\gamma^5 \gamma_\mu \not{k} \gamma_\nu \not{k}')] \\ &= \frac{1}{4E_k E_{k'}} \left[(1 + hh')(k_\mu k'_\nu + k'_\mu k_\nu - k \cdot k' g_{\mu\nu}) - i(h + h') k^\alpha k'^\beta \epsilon_{\mu\nu\alpha\beta} \right] \\ &= \frac{1 + hh'}{4} L_{\mu\nu}^{(0)} - \frac{i(h + h')}{4E_k E_{k'}} k^\alpha k'^\beta \epsilon_{\mu\nu\alpha\beta}, \end{aligned} \quad (\text{B.13})$$

where, we used the fact that

$$\text{Tr}(\gamma^5 \gamma_\mu \gamma_\nu \gamma_\alpha \gamma_\beta) = -4i \epsilon_{\mu\nu\alpha\beta}.$$

Appendix C

The Hadronic tensor

The hadronic matrix element can be written as

$$J^\mu = \sum_{s'_2} \langle p'_1; p'_2, s'_2; \Psi_f(P') | \hat{J}^\mu(q) | \Psi_i(P) \rangle, \quad (\text{C.1})$$

so that the hadronic tensor is written as:

$$W^{\mu\nu} = J^\mu (J^\nu)^*. \quad (\text{C.2})$$

where $\hat{J}^\mu(q)$ is the hadronic current given by Eq. (3.33). The approximation in chapter three [see Eq.(3.32)] leads to

$$J^\mu = \sum_{m, s'_2} \bar{U}(\mathbf{p}'_2, s'_2) \hat{J}^\mu(q) U_{\alpha, m}(\mathbf{p}_m), \quad (\text{C.3})$$

then Eq. (C.2) can be written as

$$W^{\mu\nu} = \sum_{m, s'_2} \left[\bar{U}(\mathbf{p}'_2, s'_2) \hat{J}^\mu(q) U_{\alpha, m}(\mathbf{p}_m) \right] \left[\bar{U}(\mathbf{p}'_2, s'_2) \hat{J}^\nu(q) U_{\alpha, m}(\mathbf{p}_m) \right]^*. \quad (\text{C.4})$$

$$\begin{aligned} W^{\mu\nu} &= \sum_{m, s'_2} \left[\bar{U}(\mathbf{p}'_2, s'_2) \hat{J}^\mu(q) U_{\alpha, m}(\mathbf{p}_m) \right] \left[\bar{U}(\mathbf{p}'_2, s'_2) \hat{J}^\nu(q) U_{\alpha, m}(\mathbf{p}_m) \right]^\dagger \\ &= \sum_{m, s'_2} \left[\bar{U}(\mathbf{p}'_2, s'_2) \hat{J}^\mu(q) U_{\alpha, m}(\mathbf{p}_m) \right] \left[U^\dagger(\mathbf{p}'_2, s'_2) \gamma^0 \hat{J}^\nu(q) U_{\alpha, m}(\mathbf{p}_m) \right]^\dagger \\ &= \sum_{m, s'_2} \left[\bar{U}(\mathbf{p}'_2, s'_2) \hat{J}^\mu(q) U_{\alpha, m}(\mathbf{p}_m) \right] \left[(U_{\alpha, m})^\dagger(\mathbf{p}_m) (\hat{J}^\nu(q))^\dagger (\gamma^0)^\dagger (U^\dagger)^\dagger(\mathbf{p}'_2, s'_2) \right] \\ &= \sum_{m, s'_2} \left[\bar{U}(\mathbf{p}'_2, s'_2) \hat{J}^\mu(q) U_{\alpha, m}(\mathbf{p}_m) \right] \left[(U_{\alpha, m})^\dagger(\mathbf{p}_m) (\hat{J}^\nu(q))^\dagger (\gamma^0)^\dagger (U^\dagger)^\dagger(\mathbf{p}'_2, s'_2) \right]. \end{aligned} \quad (\text{C.5})$$

But $(\gamma^0)^\dagger = \gamma^0$, $(\mathcal{U}^\dagger)^\dagger = \mathcal{U}$ and $\bar{\mathcal{U}} = \mathcal{U}^\dagger \gamma^0$ then it follows that

$$\begin{aligned}
W^{\mu\nu} &= \sum_{m, s'_2} \left[\bar{\mathcal{U}}(\mathbf{p}'_2, s'_2) \hat{J}^\mu(q) \mathcal{U}_{\alpha, m}(\mathbf{p}_m) \right] \left[(\mathcal{U}_{\alpha, m})^\dagger(\mathbf{p}_m) \gamma^0 \gamma^0 (\hat{J}^\nu(q))^\dagger \gamma^0 \mathcal{U}(\mathbf{p}'_2, s'_2) \right] \\
&= \sum_{m, s'_2} \left[\bar{\mathcal{U}}(\mathbf{p}'_2, s'_2) \hat{J}^\mu(q) \mathcal{U}_{\alpha, m}(\mathbf{p}_m) \right] \left[\bar{\mathcal{U}}_{\alpha, m}(\mathbf{p}_m) \gamma^0 (\hat{J}^\nu(q))^\dagger \gamma^0 \mathcal{U}(\mathbf{p}'_2, s'_2) \right] \\
&= \sum_{m, s'_2} \left[\bar{\mathcal{U}}(\mathbf{p}'_2, s'_2) \hat{J}^\mu(q) \mathcal{U}_{\alpha, m}(\mathbf{p}_m) \right] \left[\bar{\mathcal{U}}_{\alpha, m}(\mathbf{p}_m) \bar{\hat{J}}^\nu(q) \mathcal{U}(\mathbf{p}'_2, s'_2) \right],
\end{aligned} \tag{C.6}$$

where we define $\bar{\hat{J}}^\nu(q) = \gamma^0 (\hat{J}^\nu(q))^\dagger \gamma^0$. It follows that

$$\begin{aligned}
W^{\mu\nu} &= \sum_{m, s'_2} \left[(\bar{\mathcal{U}})_i(\mathbf{p}'_2, s'_2) (\hat{J}^\mu)_{ik}(q) (\mathcal{U}_{\alpha, m})_k(\mathbf{p}_m) (\bar{\mathcal{U}}_{\alpha, m})_\lambda(\mathbf{p}_m) (\bar{\hat{J}}^\nu)_{\lambda\sigma}(q) (\mathcal{U})_\sigma(\mathbf{p}'_2, s'_2) \right] \\
&= \sum_{s'_2} \left[\bar{\mathcal{U}}_i(\mathbf{p}'_2, s'_2) \hat{J}^\mu_{ik}(q) \sum_m (\mathcal{U}_{\alpha, m})_k(\mathbf{p}_m) (\bar{\mathcal{U}}_{\alpha, m})_\lambda(\mathbf{p}_m) \bar{\hat{J}}^\nu_{\lambda\sigma}(q) \mathcal{U}_\sigma(\mathbf{p}'_2, s'_2) \right] \\
&= \sum_{s'_2} \left[\bar{\mathcal{U}}_i(\mathbf{p}'_2, s'_2) \hat{J}^\mu_{ik}(q) (2j+1) (\not{p}_\alpha + M_\alpha)_{k\lambda} \bar{\hat{J}}^\nu_{\lambda\sigma}(q) \mathcal{U}_\sigma(\mathbf{p}'_2, s'_2) \right] \\
&= (2j+1) \left[\hat{J}^\mu_{ik}(q) (\not{p}_\alpha + M_\alpha)_{k\lambda} \bar{\hat{J}}^\nu_{\lambda\sigma}(q) \sum_{s'_2} \mathcal{U}_\sigma(\mathbf{p}'_2, s'_2) \bar{\mathcal{U}}_i(\mathbf{p}'_2, s'_2) \right] \\
&= \frac{2j+1}{2E_{p'_2}} \left[\hat{J}^\mu_{ik}(q) (\not{p}_\alpha + M_\alpha)_{k\lambda} \bar{\hat{J}}^\nu_{\lambda\sigma}(q) (\not{p}'_2 + M'_2)_{\sigma i} \right],
\end{aligned} \tag{C.7}$$

and that allows one to write it as trace

$$W^{\mu\nu} = \frac{2j+1}{2E_{p'_2}} \text{Tr} \left[\hat{J}^\mu(q) (\not{p}_\alpha + M_\alpha) \bar{\hat{J}}^\nu(q) (\not{p}'_2 + M'_2) \right]. \tag{C.8}$$

Now using the form of the quantity $\hat{J}^\mu(q)$, we can write

$$W^{\mu\nu} = \frac{2j+1}{2E_{p'_2}} \sum_{i, k=1}^6 A_i A_k^* \text{Tr} \left[\mathcal{M}_i^\mu(\not{p}_\alpha + M_\alpha) \bar{\mathcal{M}}_k^\nu(\not{p}'_2 + M'_2) \right], \tag{C.9}$$

We define

$$w_{ik}^{\mu\nu} = A_i A_k^* \text{Tr} \left[\mathcal{M}_i^\mu(\not{p}_\alpha + M_\alpha) \bar{\mathcal{M}}_k^\nu(\not{p}'_2 + M'_2) \right], \tag{C.10}$$

where the quantities \mathcal{M}_i^μ are given Eq. [(3.35a) - (3.35f)]. Then one can write

$$w_{11}^{\mu\nu} = A_1 A_1^* \text{Tr} \left[\mathcal{M}_1^\mu (\not{p}_\alpha + M_\alpha) \overline{\mathcal{M}_1^\nu} (\not{p}'_2 + M'_2) \right], \quad (\text{C.11a})$$

$$w_{12}^{\mu\nu} = A_1 A_2^* \text{Tr} \left[\mathcal{M}_1^\mu (\not{p}_\alpha + M_\alpha) \overline{\mathcal{M}_2^\nu} (\not{p}'_2 + M'_2) \right], \quad (\text{C.11b})$$

$$w_{13}^{\mu\nu} = A_1 A_3^* \text{Tr} \left[\mathcal{M}_1^\mu (\not{p}_\alpha + M_\alpha) \overline{\mathcal{M}_3^\nu} (\not{p}'_2 + M'_2) \right], \quad (\text{C.11c})$$

$$w_{14}^{\mu\nu} = A_1 A_4^* \text{Tr} \left[\mathcal{M}_1^\mu (\not{p}_\alpha + M_\alpha) \overline{\mathcal{M}_4^\nu} (\not{p}'_2 + M'_2) \right], \quad (\text{C.11d})$$

$$w_{15}^{\mu\nu} = A_1 A_5^* \text{Tr} \left[\mathcal{M}_1^\mu (\not{p}_\alpha + M_\alpha) \overline{\mathcal{M}_5^\nu} (\not{p}'_2 + M'_2) \right], \quad (\text{C.11e})$$

$$w_{16}^{\mu\nu} = A_1 A_6^* \text{Tr} \left[\mathcal{M}_1^\mu (\not{p}_\alpha + M_\alpha) \overline{\mathcal{M}_6^\nu} (\not{p}'_2 + M'_2) \right], \quad (\text{C.11f})$$

which gives

$$\begin{aligned} w_{11}^{\mu\nu} = & |A_1|^2 \times 4 \left[q^2 (p_\alpha^\mu p_2'^\nu + p_2'^\mu p_\alpha^\nu - [p_2' \cdot p_\alpha - M_\alpha M_2'] g^{\mu\nu}) \right. \\ & - (q \cdot p_\alpha) (q^\mu p_2'^\nu + p_2'^\mu q^\nu - (q \cdot p_2') g^{\mu\nu}) \\ & - (q \cdot p_2') (q^\mu p_\alpha^\nu + p_\alpha^\mu q^\nu - (q \cdot p_\alpha) g^{\mu\nu}) \\ & \left. + (p_2' \cdot p_\alpha - M_\alpha M_2') q^\mu q^\nu \right] \end{aligned} \quad (\text{C.12})$$

$$\begin{aligned} w_{12}^{\mu\nu} = & A_1 A_2^* \times 4 \left[[q \cdot p_\alpha p_2'^\mu - q \cdot p_2' p_\alpha^\nu] \right. \\ & \left. \times (q \cdot p_\alpha + q \cdot p_2') (2 p_1'^\nu - q^\nu) - (2 q \cdot p_1' - q^2) (p_\alpha^\nu + p_2'^\nu) \right] \end{aligned} \quad (\text{C.13})$$

$$\begin{aligned} w_{13}^{\mu\nu} = & A_1 A_3^* \times 4 \left[M_\alpha [q \cdot p_1' p_2'^\mu q^\nu + q \cdot p_2' q^\mu p_1'^\nu - q^2 p_2'^\mu p_1'^\nu - q \cdot p_1' q \cdot p_2' g^{\mu\nu}] \right. \\ & \left. + M_2' [q \cdot p_\alpha q^\mu p_1'^\nu + q \cdot p_1' p_\alpha^\mu q^\nu - q^2 p_\alpha^\mu p_1'^\nu - q \cdot p_\alpha q \cdot p_1' g^{\mu\nu}] \right] \end{aligned} \quad (\text{C.14})$$

$$w_{15}^{\mu\nu} = A_1 A_5^* \times 4 \left[(q \cdot p_\alpha p_2'^\mu - q \cdot p_2' p_\alpha^\nu) \times (q^2 p_1'^\nu - q \cdot p_1' q^\nu) \right] \quad (\text{C.15})$$

$$w_{16}^{\mu\nu} = A_1 A_6^* \times 4 \left[(q^2 g^{\mu\nu} - q^\mu q^\nu) \times (M_\alpha q \cdot p_2' + M_2' q \cdot p_\alpha) \right] \quad (\text{C.16})$$

$$\begin{aligned}
w_{22}^{\mu\nu} &= |A_2|^2 \left[p_\alpha \cdot p'_2 - M_\alpha M'_2 \right] \\
&\quad \times \left[(q \cdot p_\alpha + q \cdot p'_2) (2 p_1'^\mu - q^\mu) - (2 q \cdot p'_1 - q^2) (p_\alpha^\mu + p_2'^\mu) \right] \\
&\quad \times \left[(q \cdot p_\alpha + q \cdot p'_2) (2 p_1'^\nu - q^\nu) - (2 q \cdot p'_1 - q^2) (p_\alpha^\nu + p_2'^\nu) \right]
\end{aligned} \tag{C.17}$$

$$\begin{aligned}
w_{23}^{\mu\nu} &= A_2 A_3^* \times 2 \left[(q \cdot p_\alpha + q \cdot p'_2) (2 p_1'^\mu - q^\mu) - (2 q \cdot p'_1 - q^2) (p_\alpha^\mu + p_2'^\mu) \right] \\
&\quad \times \left[M_\alpha (q \cdot p'_1 p_2'^\nu - q \cdot p'_2 p_1'^\nu) + M'_2 (q \cdot p_\alpha p_1'^\nu - q \cdot p'_1 p_\alpha) \right]
\end{aligned} \tag{C.18}$$

$$\begin{aligned}
w_{25}^{\mu\nu} &= A_2 A_5^* \times 2 \left[(q \cdot p_\alpha + q \cdot p'_2) (2 p_1'^\mu - q^\mu) - (2 q \cdot p'_1 - q^2) (p_\alpha^\mu + p_2'^\mu) \right] \\
&\quad \times \left[(p_\alpha \cdot p'_2 - M_\alpha M'_2) (q^2 p_1'^\nu - q \cdot p'_1 q^\nu) \right]
\end{aligned} \tag{C.19}$$

$$\begin{aligned}
w_{26}^{\mu\nu} &= A_2 A_6^* \times 2 \left[(q \cdot p_\alpha + q \cdot p'_2) (2 p_1'^\mu - q^\mu) - (2 q \cdot p'_1 - q^2) (p_\alpha^\mu + p_2'^\mu) \right] \\
&\quad \times \left[M_\alpha (q \cdot p'_2 q^\nu - q^2 p_2'^\nu) + M'_2 (q^2 p_\alpha^\nu - q \cdot p_\alpha q^\nu) \right]
\end{aligned} \tag{C.20}$$

$$\begin{aligned}
w_{33}^{\mu\nu} &= |A_3|^2 \times 4 \left[(q \cdot p'_1)^2 \left[p_\alpha^\mu p_2'^\nu + p_2'^\mu p_\alpha^\nu - (p_\alpha \cdot p'_2 + M_\alpha M'_2) g^{\mu\nu} \right] \right. \\
&\quad - (q \cdot p'_1) \left[(q \cdot p_\alpha) (p_1'^\mu p_2'^\nu + p_2'^\mu p_1'^\nu) + (q \cdot p'_2) (p_1'^\mu p_\alpha^\nu + p_\alpha^\mu p_1'^\nu) \right] \\
&\quad + (q \cdot p'_1) (p_\alpha \cdot p'_2 + M_\alpha M'_2) \left[q^\mu p_1'^\nu + p_1'^\mu q^\nu \right] \\
&\quad \left. + \left[2 (q \cdot p_\alpha) (q \cdot p'_2) - q^2 (p_\alpha \cdot p'_2 + M_\alpha M'_2) p_1'^\mu p_1'^\nu \right] \right]
\end{aligned} \tag{C.21}$$

$$\begin{aligned}
w_{35}^{\mu\nu} &= A_3 A_5^* \times 4 \left[\left[M_\alpha (q \cdot p'_2 p_1'^\mu - q \cdot p'_1 p_2'^\mu) + M'_2 (q \cdot p_\alpha p_1'^\mu - q \cdot p'_1 p_\alpha) \right] \right. \\
&\quad \left. \times \left[(p_\alpha \cdot p'_2 - M_\alpha M'_2) (q^2 p_1'^\nu - q \cdot p'_1 q^\nu) \right] \right]
\end{aligned} \tag{C.22}$$

$$\begin{aligned}
w_{36}^{\mu\nu} = A_3 A_6^* \times 4 & \left[q^2 \left((q \cdot p_\alpha) p_1'^\mu p_2'^\nu + (q \cdot p_2') p_1'^\mu p_\alpha^\nu \right) \right. \\
& - (q \cdot p_1') q^2 \left[p_\alpha^\mu p_2'^\nu + p_2'^\mu p_\alpha^\nu - \left(p_\alpha \cdot p_2' + M_\alpha M_2' \right) g^{\mu\nu} \right] \\
& + \left[(q \cdot p_\alpha)(q \cdot p_1') p_2'^\mu + (q \cdot p_2')(q \cdot p_1') p_\alpha^\mu - 2 (q \cdot p_\alpha)(q \cdot p_2') p_1'^\mu \right] \\
& \left. - (q \cdot p_1') \left[p_\alpha \cdot p_2' + M_\alpha M_2' \right] q^\mu q^\nu \right] \tag{C.23}
\end{aligned}$$

$$w_{55}^{\mu\nu} = |A_5|^2 \times 4 \left[p_\alpha \cdot p_2' - M_\alpha M_2' \right] (q^2 p_1'^\mu - q \cdot p_1' q^\mu) (q^2 p_1'^\nu - q \cdot p_1' q^\nu) \tag{C.24}$$

$$\begin{aligned}
w_{56}^{\mu\nu} = A_5 A_6^* \times 4 & \left[(q^2 p_1'^\mu - q \cdot p_1' q^\mu) \right. \\
& \left. \times \left[M_\alpha (q \cdot p_2' q^\nu - q^2 p_2'^\nu) + M_2' (q^2 p_\alpha^\nu - q \cdot p_\alpha q^\nu) \right] \right] \tag{C.25}
\end{aligned}$$

$$\begin{aligned}
w_{66}^{\mu\nu} = |A_6|^2 \times 4 & \left[q^4 \left[p_\alpha^\mu p_2'^\nu + p_2'^\mu p_\alpha^\nu - \left(p_\alpha \cdot p_2' - M_\alpha M_2' \right) g^{\mu\nu} \right] \right. \\
& - q^2 \left[q \cdot p_\alpha (q^\mu p_2'^\nu + p_2'^\mu q^\nu) + q \cdot p_2' (q^\mu p_\alpha^\nu + p_\alpha^\mu q^\nu) \right] \\
& \left. + \left[2 q \cdot p_\alpha q \cdot p_2' + q^2 (p_\alpha \cdot p_2' - M_\alpha M_2') \right] q^\mu q^\nu \right]. \tag{C.26}
\end{aligned}$$

Bibliography

- [1] R. T. Weidner and R. L. Sells, *Elementary Modern Physics* (Library of Congress Catalog, 1970).
- [2] S. Boffi, C. Giusti, F. D. Pacati, and M. Radici, *Electromagnetic Response of Atomic Nuclei* (Clarendon Press Oxford, 1996).
- [3] W. Greiner and J. Reinhardt, *Quantum Electrodynamics* (Springer Verlag, 1992).
- [4] K. Heyde, *From Nucleons to the Atomic Nucleus* (Springer-Verlag Berlin Heidelberg New York, 1998).
- [5] F. J. Yndurain, *The Theory of Quark and Gluon Interaction* (Springer, 1999).
- [6] L. J. A. Raddad, arXiv: nucl-th/0005068 **1** (25 May 2000).
- [7] M. Benmerrouche, N. C. Mukhopadhyay, and J. F. Zhang, arXiv:hep-ph/9412248 **1** (06 Dec 1994).
- [8] S. Nakamura, T. Sato, V. Gudkov, and K. Kubodera, Phys. Rev. C **63**, 034617 (2001).
- [9] W.-M. Yao *et al.*, J. Phys. G **33**, 1 (2006).
- [10] L. J. Abu-Raddad and J. Piekarewicz, Phys. Rev. C **61**, 041604 (2002).
- [11] F. X. Lee, C. Bennhold, and L. E. Wright, Phys. Rev. C **55**, 318 (1997).
- [12] G. Knochlein, D. Drechsel, and L. Tiator, arXiv: nucl-th/9506029 **1** (29 Jun 1995).
- [13] H. Ejiri and H. Toki, *Nucleon-Hadron Many Body Systems* (Oxford Sciences Publications, 1998).

-
- [14] B. Saghai and F. Tabakin, arXiv: nucl-th/9606042 **1** (20 Jun 1996).
- [15] V. B. Belyaer, S. A. Rakityansky, S. A. Sofianos, N. Braun, and W. Sandhas, arXiv: nucl-th/9507043 **1** (28 Jul 1995).
- [16] Q. Zhao, B. Saghai, and Z. Li, arXiv: nucl-th/0011069 **2** (26 Mar 2002).
- [17] Z. Li, H. Ye, and M. Lu, Phys. Rev. C **56**, 234 (Aug 1997).
- [18] W. Peters, U. Mosel, and A. Engel, arXiv: Nucl-th/9407031 **2** (22 Mar 1995).
- [19] B. R. Martin and G. Shaw, *Particle Physics* (, 1997).
- [20] H. Ströher, Phys. Scripta. **T99**, 143 (2002).
- [21] M. Hedayati-Poor and H. S. Sherif, arXiv: nucl-th/9707009 **1** (3 Jul 1997).
- [22] I. R. Blokland and H. S. Sherif, arXiv: nucl-th/0104006 **1** (2 April 2001).
- [23] C. Elster, A. Sibirtsev, S. Schneider, and J. Haidenbauer, arXiv: nucl-th/0207052 **1** (16 Jul 2002).
- [24] B. Borasoy, arXiv: Help-ph/0102112 **1** (9 Feb 2001).
- [25] B. I. S. van der Ventel, L. J. Abu-Raddad, and G. C. Hillhouse, Phys. Rev. C **68**, 024601 (2003).
- [26] A. Sibirtsev *et al.*, arXiv: nucl-th/0111086 **1** (30 Nov 2001).
- [27] D. Halderson and A. S. Rosenthal, Phys. Rev. C **42**, 2584 (1990).
- [28] B. B. Deo and A. K. Bisoi, Phys. Rev. D **9**, 288 (1974).
- [29] C. Volpe, N. Auerbach, G. Colo, and N. V. Gial, Phys. Rev. C **65**, 044603 (2002).
- [30] G. F. Chew, M. L. Goldberg, F. E. Low, and Y. Nambu, Phys. Rev. **106**, 1345 (1957).
- [31] H. Kim, J. Piekarewicz, and C. J. Horowitz, Phys. Rev. C **51**, 2739 (1995).
- [32] G. K. Dillon, *Cinematque des Reactions Nucleaires* (Dunod, Paris, 1964).

-
- [33] Baldin, A. M., V. I. Goldansky, and I. L. Rosental, *Kinematics of Nuclear Reactions* (Pergamon Press, 1961).
- [34] A. Michalowicz, *Cinematque des Reactions Nucleaires* (Dunod, Paris, 1964).
- [35] M. W. Guidry, *Gauge field theories, An Introduction with Applications* (McGraw-Hill, New York, N.Y., 1996).
- [36] D. H. Perkins, *Introduction to High Energy Physics* (Cambridge University Press, 2000).
- [37] C. Itzykson and J. B. Zuber, *Quantum Field Theory* (McGraw-Hill, New York, N.Y., 1980).
- [38] J. D. Bjorken and S. D. Drell, *Relativistic Quantum Mechanics* (McGraw-Hill, New York, N.Y., 1965).
- [39] B. D. Serot and J. D. Walecka, *Adv. Nucl. Phys.* **16**, 1 (1986).
- [40] M. Barranco, M. Pi, S. M. Gatica, E. S. Hernandez, and J. Navarro, *Phys. Rev. B* **56**, 8997 (1997).
- [41] V. Milanovic and Z. Ikovic, *J. Phys. A* **32**, 7001 (1999).
- [42] F. Dominguez-Adame and M. A. Gonzalez, *Europhys. Lett.* **13**, 193 (1990).
- [43] A. D. Alhaidari, *Phys. Lett.* **A322**, 72 (2004).
- [44] J. Sakurai, *Advanced Quantum Mechanics* (Addison-Wesley, 1973).
- [45] J. D. Walecka, *ann. Phys. (N.Y.)* **83**, 491 (1974).
- [46] B. D. Serot, *Phys. Lett.* **87B**, 403 (1979).
- [47] B. G. Todd-Rutel and J. Piekarewicz, *arXiv:nucl-th/0504034* **1** (01 April 2005).
- [48] J. Piekarewicz, *arXiv: nucl-th/0709.2699* **1** (17 Sep 2007).
- [49] B. I. S. van der Ventel and J. Piekarewicz, *Phys. Rev. C* **69**, 035501 (2004).
- [50] T. Mart and C. Bennhold, *Phys. Rev. C* **61**, 012201 (1999).

-
- [51] R. T. Weidner and R. L. Sells, *Introduction to Elementary Particles* (John Wiley & Sons, 1987).
- [52] S. Gardner and J. Piekarewicz, Phys. Rev. C **50**, 2822 (Aug 1994).
- [53] N. Jachowicz, K. Vantournhout, J. Ryckebusch, and K. Heyde, Phys. Rev. Lett **93**, 082501 (2004).
- [54] D. S. Armstrong *et al.*, Phys. Rev. Lett **95**, 092001 (2005).
- [55] E. J. Brash, A. Kozlov, S. Li, and G. M. Huber, Phys. Rev. C **65**, 051001(R) (2002).
- [56] F. X. Lee, T. Mart, C. Bennhold, H. Haberzettl, and L. E. Wright, Nucl. Phys. **A695**, 237 (2001).
- [57] F. X. Lee, L. E. Wright, C. Bennhold, and L. Tiator, Nucl. Phys. **A603**, 345 (1996).
- [58] H. Feshbach, *Theoretical Nuclear Physics* (Wiley, New York, 1992).
- [59] A. Donnachie and G. Shaw, *Electromagnetic Interactions of Hadrons* (Plenum, New York, 1978).
- [60] L. Tiator, C. Bennhold, and S. S. Kamalov, Nucl. Phys. **A580**, 455 (1994).
- [61] D. Jido, N. Kodama, and M. Oka, Phys. Rev. D **54**, 4532 (1996).
- [62] H. Garcilazo and E. M. de Guerra, Nucl. Phys. **A562**, 511 (1993).
- [63] R. Hagedorn, *Relativistic Kinematics*. (Benjamin, New York., 1963).
- [64] M. Kirchbach and L. Tiator, arXiv: nucl-th/9601002 **1** (4 Jan 1996).
- [65] N. C. Mukhopadhyay, J. F. Zhang, and M. Benmerrouche, arXiv: help-ph/9507435 (28 Jul 1995).
- [66] M. N. Rosenbluth, Phys. Rev. **79**, 615 (1965).
- [67] W. Peters, H. Lenske, and U. Mosel, arXiv: nucl-th/9807002 **2** (22 Aug 1998).
- [68] G. T. Garvey, S. Krewald, and K. Langanke, Phys. Rev. B **289**, 249 (1992).